Journal of Medicinal Chemistry

pubs.acs.org/jmc

Article

Potent Neutralizing Antibodies Elicited by RBD-Fc-Based COVID-19 Vaccine Candidate Adjuvanted by the Th2-Skewing iNKT Cell Agonist

Xi-Feng Wang,[⊥] Meng-Jia Zhang,[⊥] Na He, Ya-Cong Wang, Cheng Yan, Xiang-Zhao Chen, Xiao-Fei Gao, Jun Guo, Rui Luo,* and Zheng Liu*

Cite This: https://doi.org/10.1021/acs.jmedchem.1c00881

Read Online

ACCESS | Metrics & More | Article Recommendations | Supporting Information

ABSTRACT: The development of a safe and effective COVID-19 vaccine is of paramount importance to terminate the current pandemic. An adjuvant is crucial for improving the efficacy of the subunit COVID19 vaccine. α-Galactosylceramide (αGC) is a classical iNKT cell agonist which causes the rapid production of Th1- and Th2-associated cytokines; we, therefore, expect that the Th1- or Th2-skewing analogues of αGC can better enhance the immunogenicity of the receptor-binding domain in the spike protein of SARS-CoV-2 fused with the Fc region of human IgG (RBD-Fc). Herein, we developed a universal synthetic route to the Th1-biasing (α-C-GC) and Th2-biasing (OCH and C20:2) analogues. Immunization of mice demonstrated that αGC-adjuvanted RBD-Fc elicited a more potent humoral response than that observed with Alum and enabled the sparing of antigens. Remarkably, at a low dose of the RBD-Fc protein (2 μg), the Th2-biasing agonist C20:2 induced a significantly higher titer of the neutralizing antibody than that of Alum.

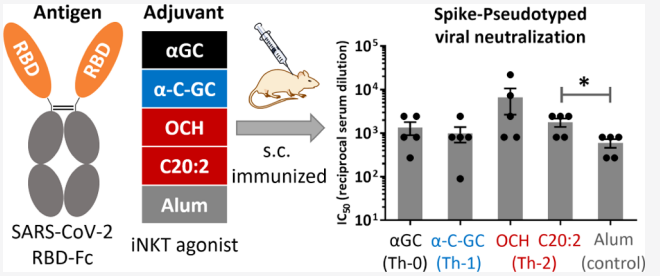

INTRODUCTION

The pandemic of coronavirus disease 2019 (COVID-19), caused by severe acute respiratory syndrome coronavirus 2 (SARS-CoV-2) infection, has led to global social and economic disruption as well as substantial healthcare challenges. The development of a safe and effective vaccine is of paramount importance to terminate this pandemic, particularly as variants of SARS-CoV-2 continue to evolve.[1] To date, various vaccine types have been developed. Compared to RNA vaccines and adenovirus vector vaccines that we have limited experience with, the protein-based subunit vaccines are well understood with a proven track record of safety and efficacy in many infectious diseases.[2]

The receptor-binding domain (RBD) in the spike (S) protein of SARS-CoV-2 mediates viral entry during the initial infection through its binding to the angiotensin-converting enzyme 2 (ACE2) receptor. The computational study showed that RBD, unlike other parts of S proteins, is not extensively shielded by glycans from antibody recognition.[3] The glycosylation sites were located in the RBD core subdomain and were found to be distant from the area bound to ACE2.[4] Wang and co-workers, through the chemical synthesis of homogeneous glycoforms of RBD, showed that the glycosylation on the RBDs does not impact their binding with ACE2.[5] Therefore, RBD serves as an important antigen for the development of COVID-19 subunit vaccines, and numerous researchers revealed the great potential of RBD-based subunit vaccines.[6−10] However, the use of RBD in vaccines is impaired by its poor immunogenicity owing to its small molecular size. In addition, RBD tends to establish a monomer−dimer equilibrium in solution by forming the disulfide bond at the cysteine residue C603, and there is a sharp difference in the immunogenicity of the RBD monomer and dimer.[6] One solution to address these limitations is to fuse the C-terminus of RBD with the Fc fragment of human IgG, generating RBD-Fc with improved *in vivo* stability and immunoglobulin-mediated effector function.[11−13] Importantly, the RBD-Fc-based vaccine can provide protection against SARS-CoV-2 with several natural mutations in RBD,[4,14,15] including the N501Y and D614G mutations. These findings are valuable concerning the emergence of SARS-CoV-2 variants globally. A recombinant vaccine containing an RBD-Fc fusion (RBD-Fc Vacc) is currently being assessed in phase I/II human clinical trials.[4]

Apart from the identification of suitable antigens, an equally crucial aspect of subunit vaccines is the selection of appropriate

Received: May 16, 2021

adjuvants,[16] which can augment the magnitude, quality, and durability of the immune responses induced by vaccination even with lower doses of the antigen. The most widely used adjuvant, an aluminum salt (Alum), has been the only human vaccine adjuvant used over the last century.[17] Substantial effort has been expended to choose a highly effective adjuvant for the RBD-based subunit COVID-19 vaccine.[18,19] α-galactosylceramide (αGC) is an invariant natural killer T (iNKT)-cell ligand whose adjuvant activity has aroused great research interest over the past 2 decades.[20] iNKT cells are a subset of T lymphocytes which are specifically activated by glycolipid antigens presented by the atypical MHC class I molecule CD1d. Upon activation, iNKT cells rapidly secrete abundant amounts of T helper (Th) 1, Th2, and Th17 cytokines and tailor the immune response through the subsequent activation of dendritic, NK, T, and B cells. As a classical iNKT glycolipid agonist, αGC demonstrates excellent immunological activity in animal models, but the elicitation of the concomitant secretion of Th1 and Th2 cytokines, which have opposing functions *in vivo*, is believed to limit the clinical outcome of αGC-based immunotherapy. Consequently, some analogues of αGC were developed that can alter the downstream cytokine response, skewing it toward either a more pronounced Th1 or a Th2 phenotype. The most extensively studied Th1-biasing agonist is α-C-GC (Scheme 1B), in which the oxygen of the glycosidic bond was replaced with a methylene group.[21] α-C-GC demonstrated a highly improved potency over αGC: a 1000-fold more potent antimalarial activity and a 100-fold more potent antimetastatic activity in the mouse models of malaria and melanoma metastases, respectively.[22] OCH, an analogue of αGC with a truncated sphingosine side chain, induces a predominant Th2 response *in vivo*.[23] C20:2 contains a C20-acyl chain with a diene and has been identified as an exceptionally potent iNKT cell activator that delivered a markedly Th2-biased cytokine response in mice and had potent anti-inflammatory properties.[24]

The adjuvant activity of αGC and analogues have been explored in the vaccines against influenza[25−28] and HIV.[29−31] Notably, αGC was shown to have a dose-sparing effect[29,32,33] and, equally important, αGC is also capable of promoting a rapid rise in serum IgG after one immunization.[34] These two properties may be valuable during a pandemic of an emerging infectious disease, such as COVID-19. Therefore, in the present study, we began the immunological study by examining the adjuvant activity of αGC in subunit vaccine candidates with different doses of the RBD-Fc protein (Scheme 1C). The efficacy of vaccine candidates was identified by SARS-CoV-2 RBD-specific humoral immune responses, particularly neutralizing antibodies that are the major immune correlates of protection. Because of an unbiased Th0-associated cytokine profile for αGC, we also determined whether the Th1- or Th2-skewing analogues of αGC can stimulate a more effective humoral immune response than αGC. Furthermore, given the fact that the delivery system of αGC plays an important role in optimizing NKT cell-based immune responses,[35] we investigated the impact of the liposomal formulation of αGC-based glycolipids on their adjuvant efficacy. On the other hand, to access the iNKT agonists needed here, we developed a universal synthetic route to αGC and the representative analogues (α-C-GC, OCH, and C20:2). The key steps involving olefin cross-metathesis, Sharpless asymmetric epoxidation, and ring opening of epoxides with an azide enable the construction of the three consecutive stereocenters in the sphingosine chain. The stereochemistry of epoxide opening was checked.

Scheme 1. RBD-Fc, iNKT Cell Agonists, and Immunization Protocol[a]

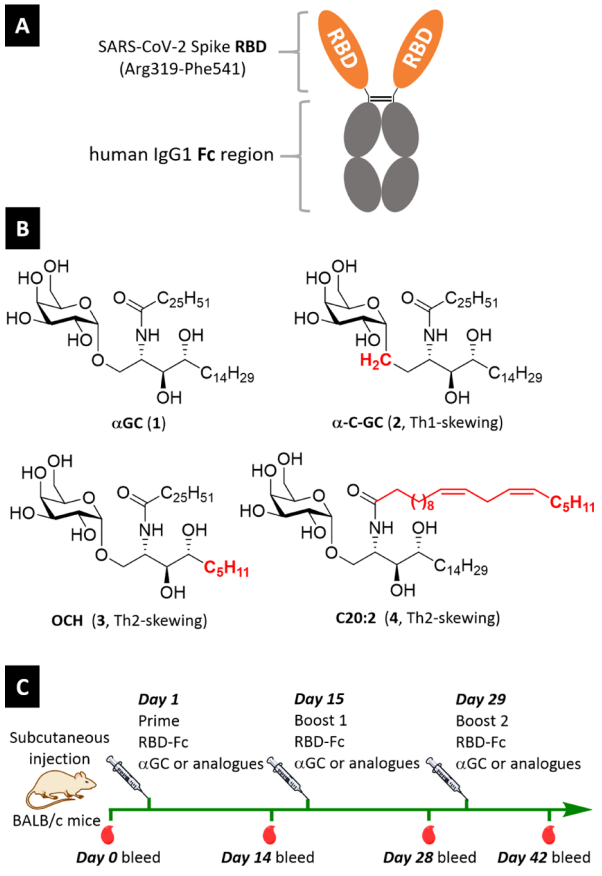

[a](A) RBD-Fc: a recombinant fusion protein generated by fusing the C-terminus of SARS-CoV-2 spike RBD to a human IgG1 Fc region. (B) Glycolipid Agonists of iNKT Cells: αGC (**1**), α-C-GC (**2**), OCH (**3**), and C20:2 (**4**). (C) Mouse immunization protocol.

RESULTS AND DISCUSSION

Synthesis of α-C-GC. Since the first synthesis of α-C-GC (**2**),[21] a variety of efficient synthetic routes have been developed due to its remarkable immunological activity.[36−43] Our current synthetic route is similar to that of α-1C-GalCer that induces Th1-biased responses in human NKT cells.[44,45] As illustrated in Scheme 2, our synthesis of **2** commenced with one-carbon homologation of **5**[46] via hydroboration, Dess−Martin oxidation, and Wittig olefination to form C-allyl glycosides **6** with 74% yield over three steps. Olefin cross-metathesis of **6** with the optically active allyl alcohol **7**[45] proceeds to afford allylic alcohol **8** after deacetylation with NaOMe. Sharpless asymmetric epoxidation[47] of **8** provides epoxy alcohol **9** with high diastereoselectivity (dr > 20:1). Chelation-controlled opening of **9** with NaN_3/NH_4Cl in aqueous MeOH under reflux delivered the desired azido diol **10** in a high yield (98%). One unidentified side product (yield < 5%) was isolated from the mixture. Notably, **10** exhibited the same R_f value to reactant **9** on the thin-layer chromatography (TLC) plate with various eluents, and the reaction progress had to be monitored with the ^{1}H NMR. The protection of diol **10** under the condition of 2,2-DMP/PPTS provides

https://doi.org/10.1021/acs.jmedchem.1c00881
J. Med. Chem. XXXX, XXX, XXX−XXX

Scheme 2. Synthesis of C-Glycoside α-C-GC (2)

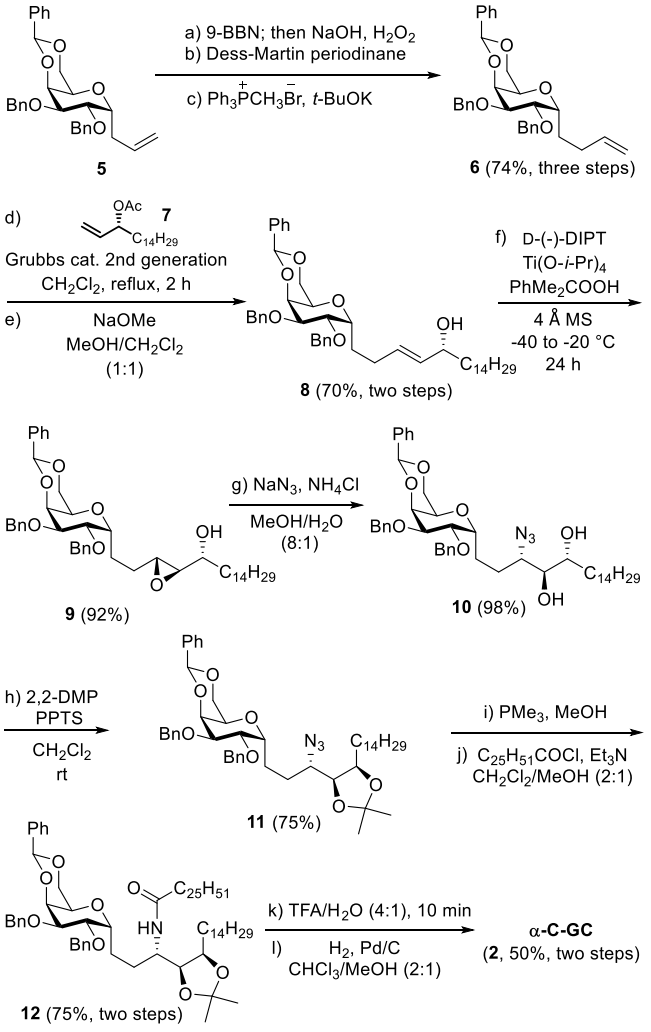

isopropylidene **11**. Subsequently, the Staudinger reduction of the azido group with PMe_3[48] and *N*-acylation with *n*-hexacosanoyl chloride afforded amide **12**, which underwent acid hydrolysis and hydrogenolysis to deliver α-C-GC (**2**).

Synthesis of αGC, OCH, and C20:2. Many synthetic routes to α-GC take the advantage of using commercially available phytosphingosine. Recently, a large-scale synthesis of α-GC has been developed.[49] However, the synthetic routes using phytosphingosine as a starting material cannot be used to prepare OCH (**3**). Given the successful preparation of α-C-GC (**2**), we carried out the synthesis of *O*-glycosides via the same synthetic sequence. As illustrated in Scheme 3, our first goal is to prepare **14** as the reactant of olefin metathesis. Owing to the toxicity of allyl alcohol, 3-bromo-1-propanol was instead employed as the glycosyl acceptor. The DMF-mediated glycosylation[50] of **13**[51] with 3-bromo-1-propanol afforded the α-glycoconjugate, which then provided the allyl galactoside **14** after elimination with *t*-BuOK. Similar to the synthesis of α-C-GC, the three-step transformation of **14** into **16-αGC** or **16-OCH** was uneventful. However, the ring opening of epoxide **16-OCH** afford the azidodiol **17-OCH**, together with an almost equal amount of regioisomers **18-OCH** that was separated with column chromatography. Analogously, the conversion of **16-αGC** to **17-αGC** also gave rise to poor regioselectivity. The vanished regioselectivity might be have a similar electron-withdrawing inductive effect on both sides of the epoxide.[52] Benzylation of **17-αGC** or **17-OCH** gave rise to **19-αGC** or **19-OCH**, respectively. After Staudinger reduction of **19-αGC** or **19-OCH**, the completion of the synthesis achieved through *N*-acylation with *n*-hexacosanoyl chloride and global deprotection to deliver α-GC (**1**) or OCH (**3**).

The synthetic route to C20:2 started from **21** that was prepared by the acidic hydrolysis of benzylidene in **20-αGC**.[53] Attempt to transform **21** into **22** within one step under the condition of H_2/Pearlmann's catalyst was unsuccessful.[54] Therefore, a two-step conversion, Staudinger reduction of **21** followed hydrogenolysis of all benzylic protecting groups, was adopted to afford **22**, which was *N*-acylated by 8,11-eicosadienoic chloride to provide C20:2 (**4**) in 65% yield over three steps.

Confirmation of the Stereochemistry of Epoxide Opening. We confirmed the configuration at C-3 by the advanced Mosher method.[55] As shown in Scheme 4A, Mosher amides were prepared by the reaction of (*S*)-(+)-α-methoxy-α-(trifluoromethyl)phenylacetic acid (MTPA) chloride or (*R*)-MTPA chloride with amine, which was prepared by the reduction of the azido group in **10**. Due to the overlap of crucial signals in the ^{1}H NMR spectrum, further derivatization was conducted to provide **24S** and **24R**. ^{1}H NMR analysis of the corresponding (*S*)- and (*R*)-Mosher amides reveals the difference between the chemical shifts of the H_a in the (*R*)- and (*S*)- MTPA ester. The upfield signal of H_a in the (*S*)-MTPA ester **24S** (δ_S = 4.99 ppm) compared to that in the (*R*)-MTPA ester **24R** (δ_R = 4.89 ppm) indicates that **10** has the *R* configuration ($\delta_{Ha} = \delta_S - \delta_R$ = +0.10 ppm) at the C-3 position. In addition, the ^{1}H and ^{13}C NMR spectra of α-C-GC prepared by our new route are identical to those of the authentic sample but are different from the C-3 epimer of α-C-GC,[56] further excluding the intramolecular participation of oxygen in the step of epoxide opening.

Fraser-Reid and Mootoo reported that oxygens present in ethers and pyranose rings can participate in electrophilic reactions at remote centers via five- and six-membered heterocycles.[57] In fact, Franck and Pu did observe the retention of configuration at the azide-bearing carbon during the step of epoxide opening by azide as a nucleophile.[56] Two mechanisms could cause the double inversion of the C-3 position (Scheme 4B): intramolecular participation by galactosyl ring oxygen (route i) or the 2′-*O*-benzyl group (route ii) to form an oxonium ion intermediate, which on an attack by the azide would form azido diol **10′** with the retention of stereoconfiguration.

Unlike the high regioselectivity in the step of epoxide opening in the synthesis of *C*-glycoside, the epoxide opening in the synthesis of the *O*-glycoside gave rise to a mixture of regioisomers. We confirmed the regiochemistry by ^{13}C NMR analysis of acetonides **25** and **26**, which were prepared by the treatment of **17-OCH** and **18-OCH** with 2,2′-dimethoxypropane (DMP), respectively. The quaternary ketal carbon signal (δ 108 and δ 101 ppm is a characteristic of a five- and six-membered acetonide, respectively)[58] unambiguously indicated the relationship of the two hydroxy groups (Scheme 4C).

αGC-Adjuvanted RBD-Fc Protein Elicited a More Potent Anti-RBD Antibody Response than Alum. To evaluate the antibody responses elicited by the αGC-adjuvanted RBD-Fc protein, we immunized BALB/c mice three times at 2 week intervals, and sera were collected on day 0 and 14 days after each vaccination, according to the protocol

https://doi.org/10.1021/acs.jmedchem.1c00881
J. Med. Chem. XXXX, XXX, XXX−XXX

Scheme 3. Synthesis of O-Glycosides: (A) α-GC (1) and OCH (3) and (B) C20:2 (4)

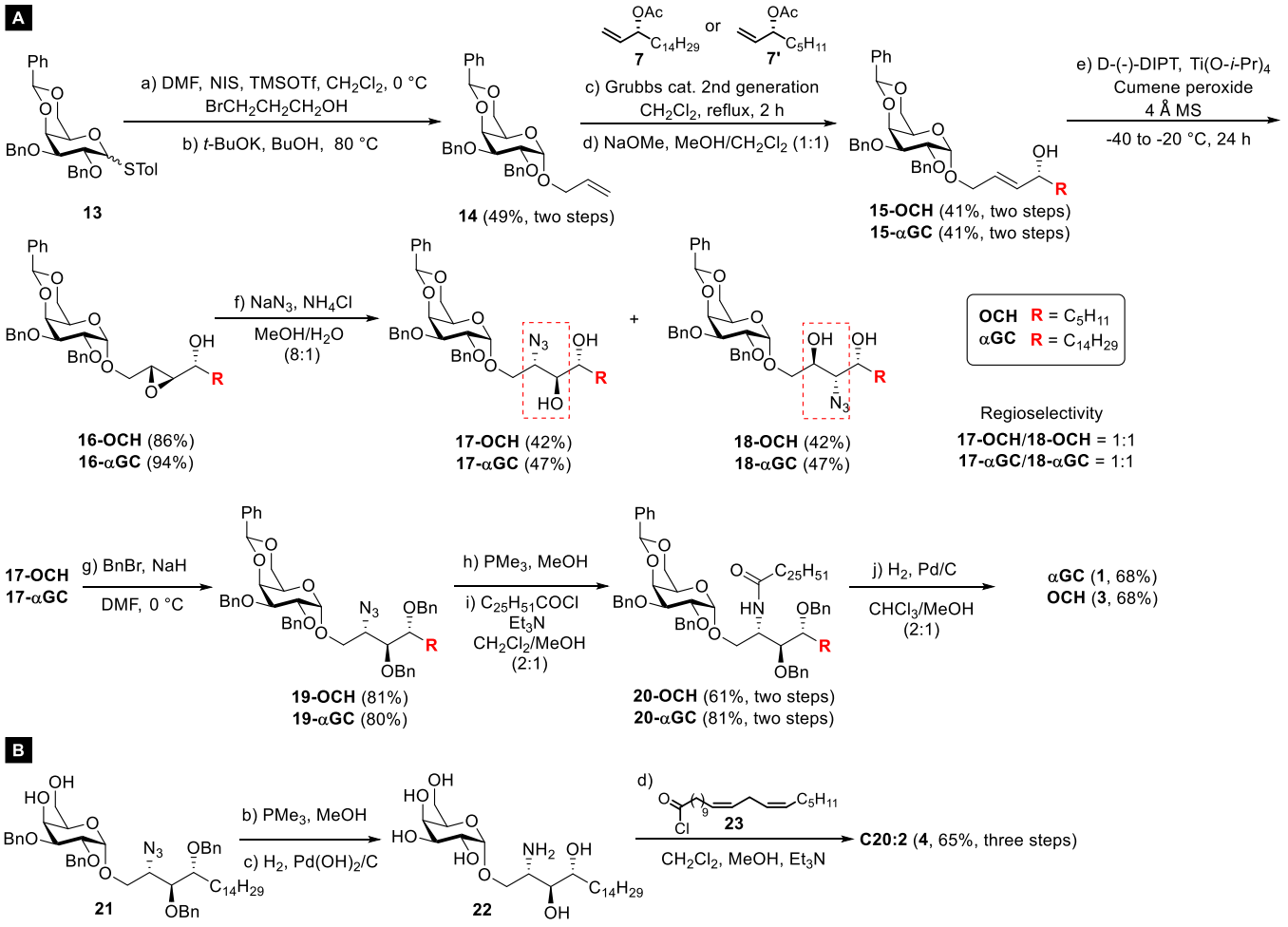

displayed in Scheme 1C. Alum was chosen as a positive control because it is a time-honored adjuvant that has been considered as the "gold standard" against which new adjuvant candidates are compared.[17] The negative control animals were administered with RBD-Fc alone. Given the global scale need for immunization against SARS-CoV-2, we sought to determine the potential for αGC to enable antigen dose sparing, three different dose levels of the RBD-Fc protein (2, 8, and 32 μg, respectively) were admixed with adjuvants (Table S2). The subcutaneous injections, rather than intraperitoneal or intravenous injections, were adopted to avoid or reduce the impact of iNKT cell anergy.[59] 2 μg of αGC was administrated because this amount will not decrease the frequency of splenic or lymph node iNKT cells.[59] Although a more potent immune response was found to be induced by cationic liposomes,[60] we chose to formulate αGC in non-cationic liposomes to avoid cytotoxicity and uncontrolled immune responses, especially regarding the high safety demand on COVID-19 vaccines.

A strong correlation has been found between spike-pseudotyped neutralization assay and protection from a SARS-CoV-2 challenge in non-human primates.[19] Neutralizing activity was assessed through the measurement of pseudovirus neutralization titers at the half-maximal inhibitory concentration (IC_{50}). As shown in Figure 1A and Table S7, analysis of the neutralizing antibody level on day 42 reveals that the αGC-adjuvanted group at the 32 and 8 μg of antigen dose levels elicit significantly enhanced neutralizing titers, at least 5-fold greater than those observed in cohorts that receive dose-matched RBD-Fc alone. Furthermore, the level of the neutralizing antibody in mice vaccinated with 8 μg of RBD-Fc in the presence of αGC was 2.3-fold higher than that in mice vaccinated with 32 μg of RBD-Fc in the absence of any adjuvant, although this difference did not reach statistical significance, indicating a significant potential for αGC to enable dose sparing of the RBD-Fc protein. In contrast, Alum induced mildly increased titers of the neutralizing antibody compared to the immunization of RBD-Fc with no adjuvant, and no statistical difference was observed between Alum and no adjuvant for all three doses of RBD-Fc. It is worth mentioning that when 32 μg of RBD-Fc was administrated, the neutralizing antibody titer was significantly higher for αGC-treated mice compared with Alum tested, suggestive of the greater adjuvant activity of αGC than Alum.

A pseudovirus neutralization assay on sera collected on day 28 indicated that the vaccination of 2 μg of the RBD-Fc protein adjuvanted by αGC achieved approximate 1450 titer of the neutralizing antibody after second immunization, although there is no statistical significance compared to other two dose-matched comparators, this same level of neutralization was accomplished by Alum with 8 μg of the RBD-Fc protein after third immunization (on day 42) or Alum with 32 μg of the RBD-Fc protein on day 28 (Figure 1A and Table S6), indicating, to some extent, the rapid production of an effective antibody response as well as dose-sparing effect offered by

https://doi.org/10.1021/acs.jmedchem.1c00881
J. Med. Chem. XXXX, XXX, XXX−XXX

Scheme 4. Confirmation of the Stereochemistry of Epoxide Opening[a]

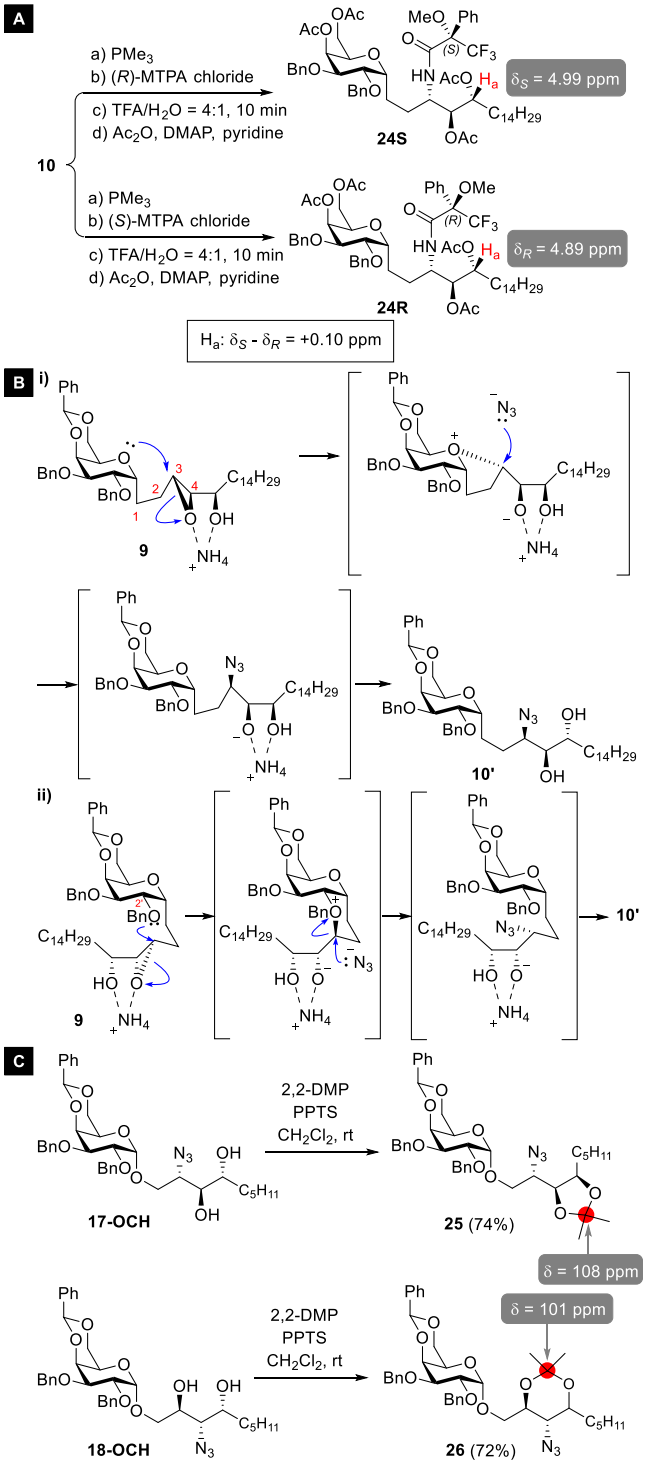

[a](A) Confirmation of the stereoconfiguration of **10** by the advanced Mosher method; (B) the possible mechanisms give rise to **10′**, the N_3 epimer of **10**, via double inversion; and (C) confirmation of the regiochemistry of **17-OCH** and **18-OCH** through the formation of dioxolane **25** and dioxane **26**.

αGC. Remarkably, the increased dose of RBD-Fc alone or combined with Alum did not induce a significantly higher level of the neutralizing antibody, consistent with the report on MERS coronavirus RBD-Fc.[61] However, αGC demonstrated a marked dose-dependent effect, probably attributable to more effective interactions between RBD-Fc and αGC.[62]

Total IgG titers were measured using the protein of RBD-His, rather than RBD-Fc, to coat the wells of plates because the immunized mice could produce anti-human Fc antibodies.[14] The IgG response exhibited similar trends to the spike-pseudotyped neutralization assay (Figure 1B). Isotype analysis gave rise to similar observations to those made against the TT antigen,[32] with αGC not significantly polarizing the Th response compared with Alum (Figure S8). Additionally, αGC induced mainly the IgG1 antibody, a trace amount of IgG2a, IgG2b, and IgG3 antibodies, being in good agreement with previous reports by Wong and co-workers.[63] However, the relatively lower level of IgG3 compared to IgG1 is in stark contrast with the similar hierarchy of IgG1 and IgG3 induced by the vaccines against carbohydrate antigens.[53,64−66] This difference might be attributed mainly to the existence of the T helper epitope in the RBD-Fc region,[67] which is contained in vaccine candidates.

RBD-Fc Protein Adjuvanted by Th2-Skewing Agonists Elicited Higher Titers of the Neutralizing Antibody. To determine whether the Th1- or Th2-skewing agonist is capable of promoting a more potent neutralizing antibody, especially in the presence of the low dose antigen, we immunized the mice with 2 μg of the RBD-Fc protein co-formulated as liposomes with 2 μg of αGC or equal mols of α-C-GC, OCH, or C20:2 (Table S3). Alum was used as a control. The anti-sera on day 42 was used to determine the level of neutralizing antibodies. As illustrated in Figure 2A,B, very high pseudovirus neutralizing antibody responses are observed in mice immunized with 2 μg of RBD-Fc adjuvanted with OCH; high responses are observed with C20:2 and αGC; and moderate responses are observed with α-C-GC and Alum. Notably, despite the magnitude being not the highest, the Th-2 skewing agonist C20:2 demonstrates a significant degree to Alum. Our data suggested that the Th2-skewing agonists, combined with a low level of the antigen, represent an optimal category of the glycolipid in stimulating the generation of neutralizing antibodies, greatly outperforming Alum.

Total IgG titers (Figure 2C) are correlated to neutralizing antibodies, except for the OCH group, probably because OCH can induce a more effective antibody affinity maturation. It is noteworthy that αGC can rapidly elicit RBD-specific IgG up to a high level of endpoint titer (~5.0×10^5) after second immunization, but the IgG level after third immunization was marginally increased (1.3-fold). In contrast, the third immunization of C20:2-treated mice can enable a 4-fold increase of the IgG level compared to the level on day 28.

To assess the Th1/Th2 bias in the IgG response elicited through immunization, we evaluated the IgG subtype profiles of our vaccine candidates (Figure 2D). Unexpectedly, the cytokine profile (IFN-γ/IL-4) of iNKT agonists is not correlated with the IgG2a/IgG1 antibody response.[68] For example, although α-C-GC mainly stimulates the production of IFN-γ (Th1 cytokine), subtypes of anti-RBD antibodies were IgG1 with a low level of IgG2a, paralleling Wong and co-workers' report on the vaccine adjuvanted by C34, a Th1-skewing iNKT agonist.[63]

The adjuvant potency of αGC can be enhanced by appropriate formulation[35] but very few studies have been devoted to examining the impact of formulation on the humoral response induced by Th1- and Th2-biasing agonists. As a result, the dimethyl sulfoxide (DMSO)-solubilized αGC,

https://doi.org/10.1021/acs.jmedchem.1c00881
J. Med. Chem. XXXX, XXX, XXX−XXX

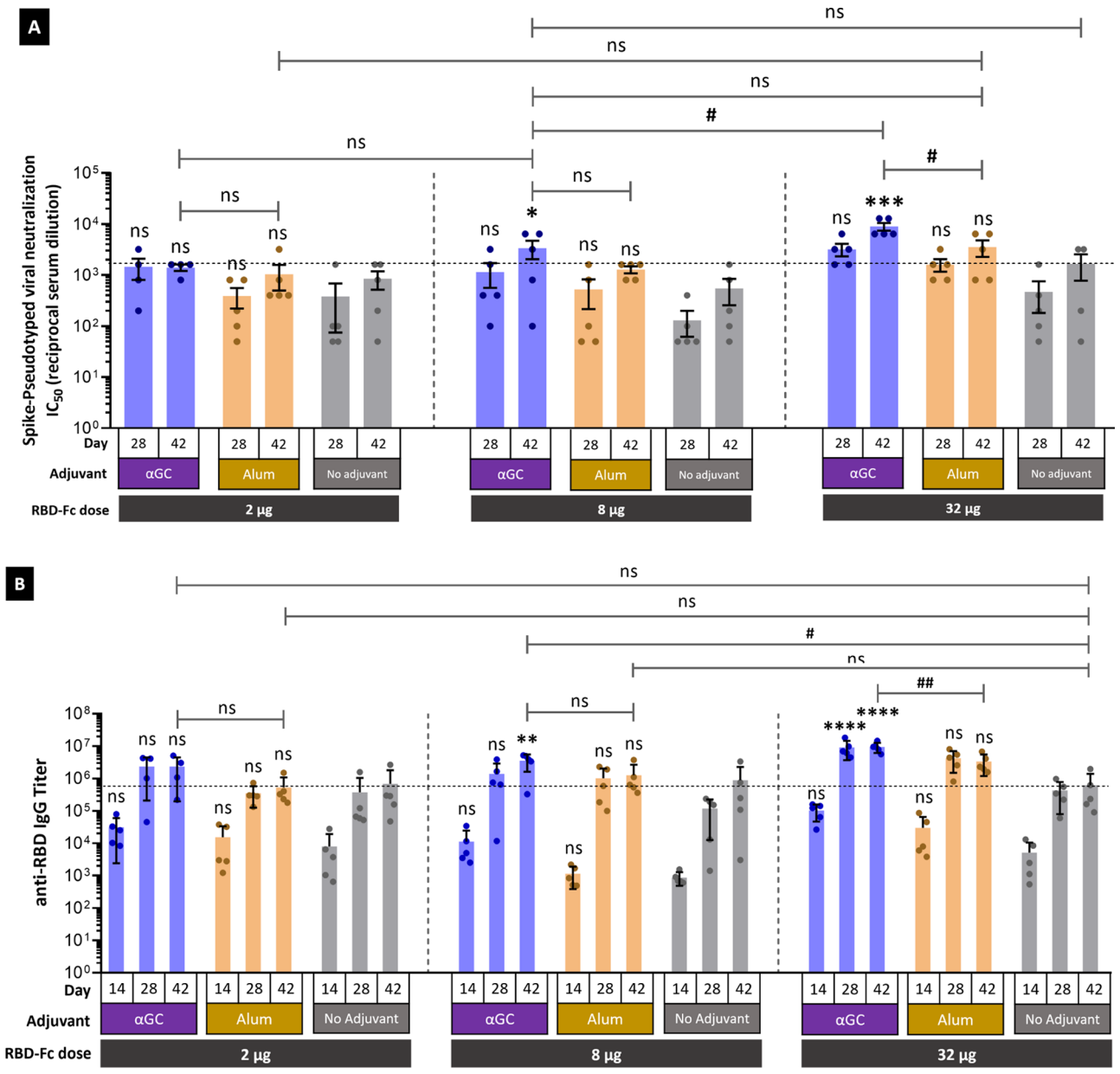

Figure 1. αGC elicits a superior neutralizing response than Alum. Female BALB/c mice (n = 4−5 per group) were immunized subcutaneously on days 1, 15, and 29 with 2, 8, and 32 μg of the Spike RBD protein admixed with 2 μg of αGC. Positive control mice were dosed with the corresponding amount of RBD-Fc admixed with 100 μL of Alum. Negative control mice were dosed with RBD-Fc alone (no adjuvant). Humoral responses specific to Spike RBD were assessed in the serum from immunized mice by the ELISA or pseudovirus neutralization assay. The data are indicated as the average ± SEM; each symbol represents one mouse serum. (**A**) IC_{50} titer of spike-pseudo-typed virus neutralization on days 28 and 42. The horizontal dashed line indicates the average IC_{50} titer with 32 μg of RBD-Fc without adjuvant on day 42. Asterisks without brackets indicate a significant difference from the dose-matched RBD-Fc without an adjuvant on day 42. (**B**) Anti-RBD IgG endpoint titers on days 14, 28, and 42. The horizontal dashed line indicates the average anti-RBD IgG titer of antisera immunized with 32 μg of RBD-Fc without an adjuvant on day 42. Asterisks without brackets indicate significant differences from the corresponding amount (2, 8, and 32 μg, respectively) of RBD-Fc without an adjuvant on day 42. Asterisks without brackets indicate the significance of multiple groups in comparison to the control group evaluated using one-way ANOVA followed by Dunnett's multiple comparison test. Pound signs with brackets indicate a significant difference calculated using unpaired two-tailed Student's t-test. ns: not significant.

α-C-GC, OCH, or C20:2 in the phosphate-buffered saline (PBS) solution were prepared and admixed with the RBD-Fc protein, respectively. Compared to the solution form, the liposomal formulation improves the adjuvant activity of all four iNKT agonists by stimulating a higher level of the anti-RBD IgG response on day 42. The increase fold is 2.0, 1.6, 3.0, and 1.4 for αGC, α-C-GC, OCH, and C20:2, respectively, and a significant difference was observed for α-C-GC (Figure 2C). Remarkably, αGC significantly elicited a higher IgG2a titer in liposomes than in solution (Figure 2D).

CONCLUSIONS

Currently, the development of safe and effective vaccines is given a high priority. Here, we synthesized iNKT glycolipid agonists (αGC, α-C-GC, OCH, or C20:2) through a universal synthetic route involving the construction of three contiguous

https://doi.org/10.1021/acs.jmedchem.1c00881
J. Med. Chem. XXXX, XXX, XXX−XXX

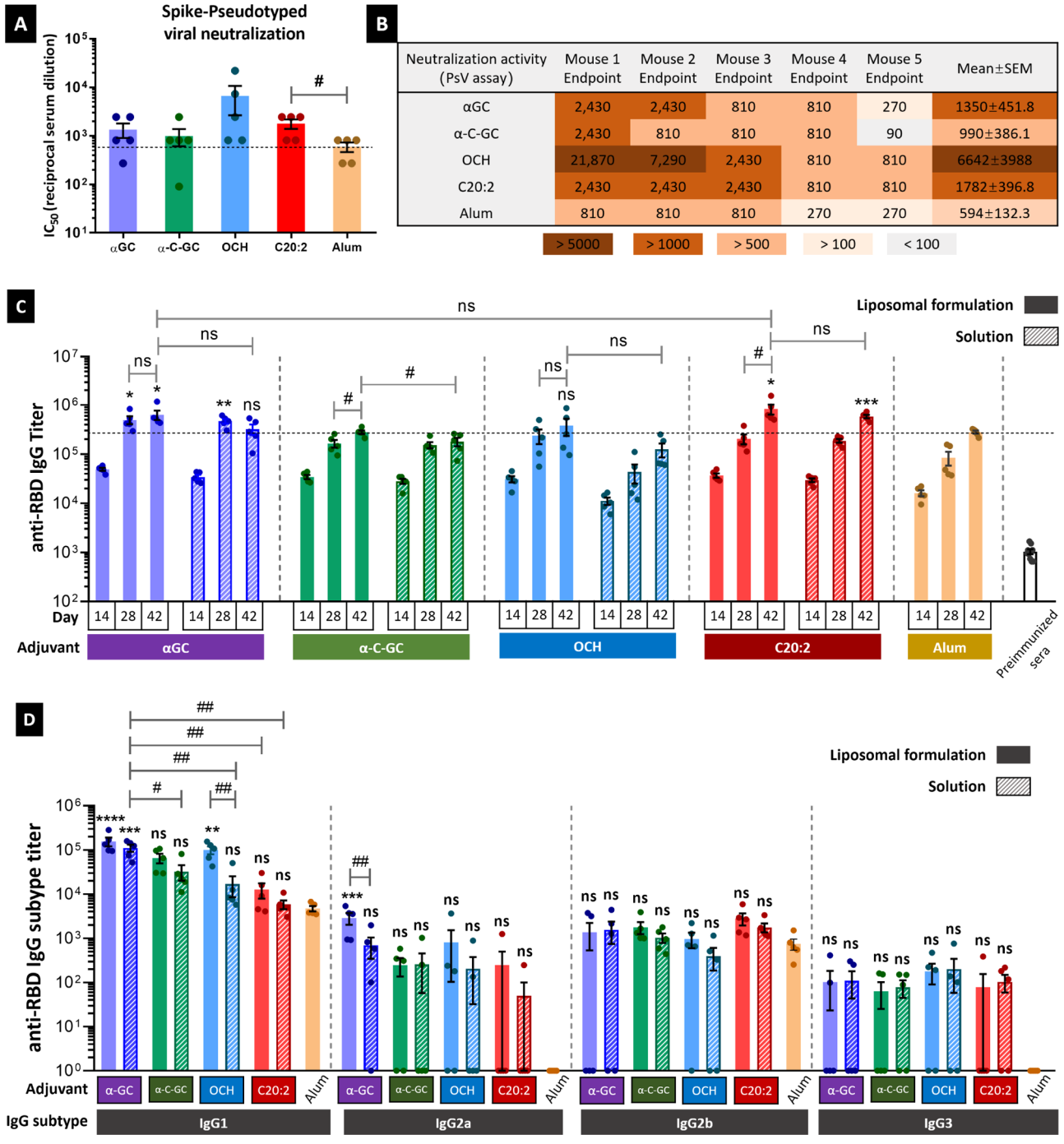

Figure 2. RBD-Fc adjuvanted by Th2-skewing agonists elicits a stronger neutralizing response than those by αGC and α-C-GC. Female BALB/c mice (n = 5 per group) were subcutaneously immunized on days 1, 15, and 29 with 2 μg of the RBD-Fc protein admixed with 2 μg of αGC or equal mols of other glycolipids (α-C-GC, OCH, or C20:2) as either a liposomal or solution form. Control mice were dosed with 2 μg of the RBD-Fc protein admixed with 100 μL of Alum. Antibody responses specific to RBD were assessed in antisera from immunized mice by the ELISA or pseudovirus neutralization assay. The data are indicated as the average ± SEM; each symbol represents one mouse serum. (**A**,**B**) IC_{50} titer of spike-pseudo-typed virus neutralization on day 42. The horizontal dashed line indicates the average neutralizing antibody titer of antisera immunized with 2 μg of RBD-Fc admixed with Alum on day 42. The deeper red color in the table represents a higher dilution ratio. (**C**) Anti-RBD IgG endpoint titers on days 14, 28, and 42. The horizontal dashed line indicates the average anti-RBD IgG titer of antisera immunized with 2 μg of RBD-Fc admixed with Alum on day 42. Asterisks without brackets indicate a significant difference to control RBD-Fc/Alum on day 42. (**D**) Anti-RBD IgG subclasses (IgG1, IgG2a, IgG2b, and IgG3) on day 42. Asterisks without brackets indicate a significant difference from the corresponding IgG subclass titer elicited by RBD-Fc/Alum on day 42. The antibody titer below the limit of detection was set to 1. Asterisks without brackets indicate the significance of multiple groups in comparison to the control group evaluated using one-way ANOVA followed by Dunnett's multiple comparison test. Pound signs with brackets indicate the significant difference calculated using unpaired two-tailed Student's t-test. ns: not significant.

https://doi.org/10.1021/acs.jmedchem.1c00881
J. Med. Chem. XXXX, XXX, XXX−XXX

stereocenters in the phytosphingosine chain. The stereoconfiguration and regiochemistry in the step of epoxide opening were confirmed. The low regioselectivity in the *O*-glycosides compared to the C-glycoside could be rationalized by the electron-withdrawing inductive effect caused by glycosidic oxygen which has been investigated by Sharpless and Behrens;[52] therefore, this parallel comparison may serve as a cautionary note for organic synthesis involving the ring opening of 2,3-epoxy alcohols under the condition of NH_4Cl/NaN_3.

Next, we demonstrated that αGC-adjuvanted RBD-Fc of high dose (32 μg) induced a significantly stronger humoral response, particularly neutralizing antibodies, than that observed with Alum. In the low dose (2 μg), the Th2-biasing glycolipids stimulated the most robust neutralizing antibody responses among the four evaluated iNKT agonists, significantly outperforming Alum. The potent adjuvant activity of OCH and C20:2 exhibited here is in line with the report by Kang and co-workers,[26] which may be explained by their improved solubility over αGC.[69] Of note, the antibody response induced by α-C-GC is statistically equal to the other glycolipid agonists, consistent with literature precedents in C57BL/6 mice[59] and pigs.[70] In addition to neutralizing antibodies, T-cell responses also play critical protective roles in SARS-CoV-2 infections.[71] Given a discordance between virus-specific antibody levels and T-cell responses[71] as well as an effective antitumor T-cell immunity triggered by α-C-GC,[72] the Th1-biasing agonist could be a potent adjuvant for T-cell responses in COVID-19 vaccines. The studies of the cellular immune response of iNKT cell agonists are in progress.

In addition to enhancing the immunogenicity of the RBD-Fc protein, αGC-based glycolipids provide practical advantages in terms of the COVID-19 pandemic, as it enables a significant reduction in the antigen dose. Considering the facile manufacturing of the recombinant RBD-Fc protein and αGC-based glycolipids on a large scale, as well as the safety profile of αGC demonstrated in clinical trials,[73,74] our data support the continued development of RBD-Fc formulated with the iNKT glycolipid agonist as a candidate vaccine to prevent the COVID-19 disease.

EXPERIMENTAL SECTION

Chemistry. *General Information.* All reactions were carried out under a dry Ar atmosphere using oven-dried glassware and magnetic stirring. The solvents were dried before use as follows: toluene, tetrahydrofuran (THF), and Et_2O were heated at the reflux over sodium; dichloromethane (DCM) was dried over CaH_2. Anhydrous *N*,*N*-diisopropylethylamine (DIPEA) and triethylamine were used directly as purchased. Commercially available reagents were used without further purification unless otherwise noted. Reactions were monitored by analytical TLC on silica gel 60 × 10^{254} glass plates. The spots were visualized with short wavelength UV light or by charring after spraying with a solution prepared from one of the following solutions: phosphomolybdic acid (5.0 g) in 95% EtOH (100 mL); *p*-anisaldehyde solution (2.5 mL of *p*-anisaldehyde, 2 mL of AcOH, and 3.5 mL of concentrated H_2SO_4 in 100 mL of 95% EtOH); or ninhydrin solution (0.3 g of ninhydrin was dissolved in 100 ml of *n*-butanol and 3 mL of AcOH was added). Flash chromatography was carried out with silica gel 60 (230−400 ASTM mesh). NMR spectra were obtained on a 400 or 600 MHz spectrometer. Proton chemical data are reported as follows: chemical shift, multiplicity (s = singlet, d = doublet, t = triplet, q = quartet, m = multiplet, br = broad), coupling constant, and integration. Chemical shifts were referenced to residual solvent peaks: $CDCl_3$ (δ = 7.26 ppm for ^{1}H NMR and 77.00 ppm for ^{13}C NMR), CD_2Cl_2 (δ = 5.32 ppm for ^{1}H NMR and 53.84 ppm for ^{13}C NMR), and CD_3OD (δ = 3.31 ppm for ^{1}H NMR and 49.00 ppm for ^{13}C NMR). Electrospray ionization (ESI) mass was obtained on a Thermo Scientific Ultimate 3000/TSQ Quantum access MAX. The high-performance liquid chromatography system (HPLC) employed was an Agilent 1260 fitted with an evaporative light scattering detector (ELSD) detector. The purities of αGC, α-C-GC, OCH, and C20:2 are >95%, as determined by HPLC-ELSD (see the Supporting Information).

*1-(But-3-en-1-yl)-2,3-bis-O-(benzyloxy)-4,6-O-(phylmethyiene)-α-C-D-galactopyranoside (**6**).* To the solution of **5** (3.27 g, 6.93 mmol) in anhydrous THF (70 mL) was added 9-BBN (0.5 M solution in THF, 27.7 mL, 13.86 mmol) at rt. After 3 h of stirring at rt, EtOH (28.0 mL), H_2O_2 (38 mL, 296.59 mmol), and 30% aqueous solution of NaOH (9.3 mL) were added at 0 °C, and the resulting mixture was stirred at rt for 1 h, then treated with 100 mL saturated aqueous NaCl solution. The organic layer was separated, and the aqueous layer was extracted with Et_2O. The combined organic phase was dried ($MgSO_4$) and concentrated under reduced pressure. The resulting residue was purified by flash column chromatography (petroleum ether/ethyl acetate = 1:1) on silica gel to provide the primary alcohol (3.24 g, 95%) as colorless oil. **^{1}H NMR** (400 MHz, $CDCl_3$): δ 7.54 (d, J = 7.1 Hz, 2H), 7.34 (m, 13H), 5.49 (s, 1H), 4.92−4.52 (m, 4H), 4.28−4.16 (m, 4H), 4.00 (d, J = 12.5 Hz, 1H), 3.75 (m, 1H), 3.69 (d, J = 5.7 Hz, 1H), 3.64 (d, J = 5.9 Hz, 1H), 3.45 (s, 1H), 1.80 (d, J = 12.6 Hz, 1H), 1.74−1.64 (m, 1H), 1.62 (d, J = 9.9 Hz, 2H). **^{13}C NMR** (100 MHz, $CDCl_3$): δ 138.7, 138.6, 137.9, 129.0, 128.4, 128.4, 128.2, 127.8, 127.7, 126.4, 101.2, 76.6, 75.8, 75.3, 74.6, 73.7, 71.7, 70.0, 63.1, 62.6, 29.3, 21.0. **MS** (ESI): calcd for $C_{30}H_{34}NaO_6^+$ $[M + Na]^+$, 513.22; found, 513.25. The alcohol obtained (2.20 g, 4.48 mmol) was dissolved in CH_2Cl_2 (50 mL) and treated with $NaHCO_3$ (1.13 g, 13.44 mmol) and Dess−Martin periodinane (5.70 g, 13.44 mmol) at 0 °C. The reaction mixture was stirred for 1 h at rt, and then quenched with aqueous solution of $Na_2S_2O_3$ and $NaHCO_3$. The biphasic mixture was stirred for 15 min and extracted with ethyl acetate (2 × 70 mL). The combined organic layers were washed with H_2O (2 × 20 mL) and brine (40 mL), dried (anhydrous Na_2SO_4), and concentrated under reduced pressure. Purification of the residue by flash column chromatography (petroleum ether/ethyl acetate = 3:1) on silica gel provided the aldehyde as a white solid (1.85 g, 85%). **^{1}H NMR** (400 MHz, $CDCl_3$) δ 9.80 (s, 1H), 7.59−7.44 (m, 2H), 7.44−7.24 (m, 13H), 5.47 (s, 1H), 4.95−4.56 (m, 4H), 4.22 (m, 1H), 4.18 (d, J = 3.3 Hz, 1H), 4.14 (m, 1H), 4.10 (m, 1H), 3.96 (m, 1H), 3.74 (m, 1H), 3.37 (s, 1H), 2.63−2.39 (m, 2H), 2.02 (m, 1H), 1.94 (m, 1H). **^{13}C NMR** (100 MHz, $CDCl_3$) δ 201.9, 138.6, 138.4, 137.7, 128.8, 128.3, 128.3, 128.0, 127.6, 127.6, 127.5, 126.3, 101.1, 76.4, 75.4, 75.0, 74.4, 73.7, 71.6, 69.8, 62.9, 40.6, 17.5. **MS** (ESI): calcd for $C_{30}H_{32}NaO_6^+$ $[M + Na]^+$, 511.21; found, 511.25. To a flask containing methyltriphenylphosphonium bromide (8.62 g, 24.12 mmol) and THF (80 mL) was added *t*-BuOK (2.62 g, 23.32 mmol) at 0 °C. The reaction was stirred for 30 min. A solution of the aldehyde prepared above (3.93 g, 8.04 mmol) in THF (7 mL) was added dropwise into the reaction, and the mixture was stirred for 2 h at rt. A saturated aqueous NH_4Cl solution (50 mL) was added to quench the reaction, and the reaction was extracted with ethyl acetate. The organic layer was washed with brine and dried over anhydrous Na_2SO_4. The combined organic layers were dried (Na_2SO_4) and concentrated under reduced pressure, and the residue was purified with flash column chromatography (petroleum ether/ethyl acetate = 10:1 to 7:1) affording product **6** (3.39 g, 87%) as a white solid. **^{1}H NMR** (400 MHz, $CDCl_3$): δ 7.78−7.45 (m, 2H), 7.42−7.25 (m, 13H), 6.01−5.70 (m, 1H), 5.49 (s, 1H), 5.11−5.01 (m, 1H), 4.97 (d, J = 10.1 Hz, 1H), 4.87−4.59 (m, 4H), 4.31−4.15 (m, 4H), 4.06−3.93 (m, 1H), 3.75 (m, 1H), 3.41 (s, 1H), 2.28−2.13 (m, 1H), 2.13−1.98 (m, 1H), 1.81 (m, 1H), 1.69 (s, 1H). **^{13}C NMR** (100 MHz, $CDCl_3$): δ 138.7, 138.6, 138.0, 137.8, 128.7, 128.2, 128.2, 128.0, 127.5, 127.5, 127.5, 127.4, 126.3, 114.9, 101.0, 76.6, 75.6, 74.5, 74.4, 73.4, 71.5, 69.9, 62.8, 29.8, 23.5. **MS** (ESI): calcd for $C_{31}H_{34}NaO_5^+$ $[M + Na]^+$, 509.23; found, 509.23.

*(5′R,3′E)-5′-Hydroxy-3′-octadecenyl-2,3-bis-O-(benzyloxy)-4,6-O-(phylmethyiene)-α-C-D-galactopyranoside (**8**).* To a solution of **6**

https://doi.org/10.1021/acs.jmedchem.1c00881
J. Med. Chem. XXXX, XXX, XXX−XXX

(1.50 g, 3.09 mmol) and **7** (1.83 g, 6.18 mmol) in CH_2Cl_2 (30 mL) was added Grubbs second generation catalyst (394 mg, 0.46 mmol, 15 mol %). The reaction mixture was stirred for 2 h at reflux under Ar and then reduced in volume to 1 mL. Purification by flash column chromatography on silica gel (petroleum ether/ethyl acetate = 8:1) provided acetate-protected alcohol (1.91 g, 82%) as a white solid. **^{1}H NMR** (400 MHz, $CDCl_3$): δ 7.54 (m, 2H), 7.47−7.12 (m, 13H), 5.71 (m, 1H), 5.49 (s, 1H), 5.41 (m, 1H), 5.16 (q, J = 6.9 Hz, 1H), 4.85−4.58 (m, 4H), 4.21 (m, 4H), 4.00 (d, J = 12.2 Hz, 1H), 3.74 (m, 1H), 3.40 (s, 1H), 2.25−2.11 (m, 1H), 2.04 (s, 4H), 1.84−1.72 (m, 1H), 1.65 (m, 1H), 1.52 (t, J = 6.8 Hz,1H), 1.25 (s, 24H), 0.88 (t, J = 6.7 Hz, 3H). **^{13}C NMR** (100 MHz, $CDCl_3$): δ 170.4, 138.7, 138.6, 137.8, 133.0, 129.1, 128.8, 128.3, 128.1, 127.6, 127.6, 127.5, 126.4, 101.1, 75.6, 74.8, 74.6, 73.5, 71.6, 69.9, 62.9, 34.5, 31.9, 29.7, 29.6, 29.6, 29.5, 29.4, 29.3, 28.5, 25.2, 23.7, 22.7, 21.4, 14.1. **MS** (ESI): calcd for $C_{48}H_{66}NaO_7^+$ $[M + Na]^+$, 777.47; found, 777.60. To a solution of the acetate-protected alcohol (77 mg, 0.098 mmol) in anhydrous MeOH (2 mL) was added 0.034 M MeONa (1.8 mL in MeOH, freshly prepared by the addition of sodium metal to MeOH) at rt, and the reaction mixture was stirred at rt for 3 h. The mixture was concentrated under reduced pressure. Purification by flash column chromatography on silica gel (petroleum ether/ethyl acetate = 4:1) provided **8** (59.3 mg, 85%) as a white solid. **^{1}H NMR** (400 MHz, $CDCl_3$): δ 7.64−7.47 (m, 2H), 7.47−7.19 (m, 13H), 5.65 (m, 1H), 5.50 (d, J = 9.6 Hz, 2H), 4.91−4.53 (m, 4H), 4.22 (d, J = 8.2 Hz, 4H), 4.01 (d, J = 11.2 Hz, 2H), 3.80−3.66 (m, 1H), 3.41 (s, 1H), 2.17 (s, 1H), 2.11−1.94 (m, 1H), 1.77 (d, J = 8.4 Hz, 1H), 1.69 (s,1H), 1.53−1.43 (m, 2H), 1.25 (s, 24H), 0.88 (t, J = 6.6 Hz,3H). **^{13}C NMR** (100 MHz, $CDCl_3$): δ 138.7, 138.5, 137.8, 133.7, 130.8, 128.8, 128.3, 128.3, 128.1, 127.6, 127.6, 127.5, 127.5, 126.3, 101.1, 75.8, 74.5, 74.4, 73.6, 73.0, 71.5, 70.0, 62.9, 37.3, 31.9, 29.7, 29.6, 29.5, 29.3, 28.2, 25.5, 24.0, 22.7, 14.1. **MS** (ESI): calcd for $C_{46}H_{64}NaO_6^+$ $[M + Na]^+$, 735.4601; found, 735.4568.

*(3′R,4′R,5′R)-1-(3′,4′-Oxiran-5′-hydroxyoctadecyl)-2,3-bis-O-(benzyloxy)-4,6-O-(phylmethyiene)-α-C-D-galactopyranoside (**9**).* A mixture of activated 4 Å molecular sieves (0.5 g), D-(−)-DIPT (382 μL, 1.81 mmol) and CH_2Cl_2 (30 mL) was stirred at rt for 30 min. After the mixture was cooled to −40 °C, Ti(O-*i*Pr)$_4$ (443 μL, 1.50 mmol) was added. After the resultant mixture was allowed to stir at −40 °C for 1 h, a solution of **8** (1.07 g, 0.291 mmol) in 6 mL of CH_2Cl_2 was added dropwise. The reaction mixture was stirred at −40 °C for another 30 min, and cumene hydroperoxide (1.04 mL, 5.99 mmol, 85%) was added via a syringe. The reaction mixture was stored at −20 °C without stirring for 24 h. Then, the mixture was filtered through a pressed pad of Celite, and to the filtrate was added 11% aqueous citric acid solution (20 mL), the mixture was stirred vigorously at rt for 30 min, and the biphasic mixture was separated. The aqueous layer was extracted with CH_2Cl_2 (3 × 20 mL). The combined organic layers were dried (Na_2SO_4) and concentrated under reduced pressure. Purification of the residue by flash chromatography on silica gel (petroleum ether/ethyl acetate = 4:1) afforded epoxy alcohol **9** (1.00 g, 92%) as a white solid. **^{1}H NMR** (400 MHz, $CDCl_3$): δ 7.63−7.48 (m, 2H), 7.45−7.14 (m, 13H), 5.49 (s, 1H), 4.91−4.51 (m, 4H), 4.28−4.10 (m, 4H), 3.99 (d, J = 12.3 Hz, 1H), 3.81−3.67 (m, 2H), 3.40 (s, 1H), 3.02 (s, 1H), 2.79 (t, J = 2.8 Hz, 1H), 1.99−1.68 (m, 1H), 1.66−1.38 (m, 6H), 1.25 (s, 24H), 0.88 (t, J = 6.7 Hz, 3H). **^{13}C NMR** (100 MHz, $CDCl_3$): δ 138.7, 138.5, 137.8, 128.9, 128.3, 128.3, 128.1, 127.6, 127.6, 126.3, 101.1, 76.5, 75.6, 74.6, 74.5, 73.7, 71.6, 69.9, 68.7, 62.9, 61.2, 54.6, 33.6, 31.9, 29.7, 29.6, 29.3, 28.1, 25.3, 22.7, 21.1, 14.1. **MS** (ESI): calcd for $C_{46}H_{64}NaO_7^+$ $[M + Na]^+$, 751.4550; found, 751.4539.

*(3′S,4′S,5′R)-1-(3′-Azido-4′,5′-dihydroxyoctadecyl)-2,3-bis-O-(benzyloxy)-4,6-O-(phylmethyiene)-α-C-D-galactopyranoside (**10**).* NH_4Cl (159 mg, 3.0 mmol) and NaN_3 (535 mg, 8.24 mmol) were added to epoxy alcohol **9** (200 mg, 0.27 mmol) in MeOH/H_2O (8:1, 9 mL). The reaction mixture was heated in a sealed tube for 24 h. The reaction mixture was allowed to cool to rt and 10 mL of water was added. The resulting mixture was extracted with CH_2Cl_2 (2 × 10 mL). The combined organic layers was dried (Na_2SO_4) and concentrated to provide azido diol **10** (203.8 mg, 98%) as a light-yellow solid, which was not purified further by flash column chromatography. **^{1}H NMR** (400 MHz, $CDCl_3$): δ 7.54 (d, J = 7.0 Hz, 2H), 7.46−7.14 (m, 13H), 5.49 (s, 1H), 4.93−4.52 (m, 4H), 4.22 (m, 4H), 4.01 (d, J = 12.7 Hz, 1H), 3.74 (d, J = 12.1 Hz, 1H), 3.61 (s, 1H), 3.46 (s, 1H), 1.96 (s, 2H), 1.77−1.39 (m, 2H), 1.26 (s, 24H), 0.88 (t, J = 6.6 Hz,3H). **^{13}C NMR** (100 MHz, $CDCl_3$) 138.6, 138.5, 137.7, 128.9, 128.3, 128.1, 127.8, 127.7, 127.6, 126.3, 101.1, 76.5, 75.8, 75.6, 74.5, 73.6, 72.1, 71.6, 69.9, 63.1, 31.9, 31.4, 29.7, 29.6, 29.6, 29.3, 26.7, 25.6, 22.7, 20.5, 14.1. **MS** (ESI): calcd for $C_{46}H_{65}N_3NaO7^+$ $[M + Na]^+$, 794.4720; found, 794.4713.

*(3′S,4′S,5′R)-1-(3′-Azido-4′,5′-(2,2-dimethyl-1,3-dioxolane)-octadencyl)-2,3-bis-O-(benzyloxy)-4,6-O-(phylmethyiene)-α-C-D-galactopyranoside (**11**).* To a solution of diol **10** (545 mg, 0.706 mmol) in anhydrous CH_2Cl_2 (6 mL) was added 2,2-DMP (886 μL, 7.06 mmol) followed by PPTS (18 mg, 0.0706 mmol). After the reaction mixture was stirred at rt for 1.5 h, the saturated $NaHCO_3$ (10 mL) was added, and the mixture was extracted with CH_2Cl_2 (3 × 20 mL). The combined organic phases were dried over Na_2SO_4. After evaporation of the solvent under reduced pressure, the residue was purified by flash column chromatography (petroleum ether/ethyl acetate = 9:1) to give product **11** (430.5 mg, 75%) as a colorless solid. **^{1}H NMR** (400 MHz, $CDCl_3$): δ 7.55 (d, J = 6.8 Hz, 2H), 7.45−7.10 (m, 13H), 5.50 (d, J = 2.5 Hz, 1H), 4.93−4.56 (m, 4H), 4.21 (q, J = 11.0, 7.6 Hz, 4H), 4.12 (s, 1H), 4.01 (d, J = 12.6 Hz, 1H), 3.87 (t, J = 7.5 Hz, 1H), 3.74 (d, J = 9.2 Hz, 1H), 3.45 (d, J = 13.8 Hz, 2H), 1.99 (d, J = 12.0 Hz, 2H), 1.70 (s, 2H), 1.51 (s, 4H), 1.39 (d, J = 2.5 Hz, 3H), 1.32 (d, J = 2.4 Hz, 3H), 1.26 (d, J = 2.5 Hz, 24H), 0.88 (m, 3H). **^{13}C NMR** (100 MHz, $CDCl_3$): δ 138.7, 138.6, 137.8, 128.3, 128.3, 128.1, 127.6, 127.6, 126.3, 108.1, 101.2, 78.0, 77.8, 76.6, 75.6, 75.6, 74.6, 73.6, 71.7, 69.9, 63.1, 60.1, 31.9, 29.7, 29.6, 29.6, 29.3, 28.1, 26.3, 25.7, 22.7, 19.5, 14.1. **MS** (ESI): calcd for $C_{49}H_{69}N_3NaO_7^+$ $[M + Na]^+$, 834.5033; found, 834.5021.

*(3′S,4′S,5′R)-1-(3′-N-n-Hexacosanoyl Acyl-4′,5′-(2,2-dimethyl-1,3-dioxolane)-octadencyl)-2,3-bis-O-(benzyloxy)-4,6-O-(phylmethyiene)-α-C-D-galactopyranoside (**12**).* PMe_3 (0.5 mL, 0.50 mmol) was added to a solution of **11** (24.8 mg, 0.031 mmol) in wet MeOH (2 mL) at rt, and the resulting solution was stirred for 2 h. Then, the solvent was concentrated under reduced pressure. The residue was then subjected to high vacuum at rt for 3 h. The crude amine was used in the next step without further purification. To the solution of the crude amine in a mixture solvent CH_2Cl_2/MeOH (2:1, 3 mL) was added Et_3N (0.5 mL) followed by the solution of the freshly prepared *n*-hexacosanoyl acid chloride **11** (0.062 mmol, in 2 mL CH_2Cl_2) at 0 °C. The mixture was stirred at rt for 30 min, quenched with saturated aqueous NH_4Cl solution and extracted with CH_2Cl_2 (3 × 30 mL). The combined organic layers were dried (Na_2SO_4) and concentrated. The resulting residue was purified by flash column chromatography (petroleum ether/ethyl acetate = 3:1) to give **12** (27 mg, 75%). **^{1}H NMR** (400 MHz, $CDCl_3$): δ 7.54 (d, J = 6.9 Hz, 2H), 7.33 (m, 13H), 5.47 (s, 1H), 5.37 (d, J = 9.4 Hz, 1H), 4.92−4.50 (m, 4H), 4.20 (m, 3H), 4.11 (d, J = 6.6 Hz, 1H), 3.99 (d, J = 11.7 Hz, 2H), 3.73 (m, 1H), 3.42 (s, 1H), 2.10 (q, J = 6.5 Hz, 2H), 1.42 (s, 3H), 1.25 (s,78H), 0.88 (t, J = 6.7 Hz, 6H). **^{13}C NMR** (100 MHz, $CDCl_3$): δ 172.6, 138.8, 138.6, 137.8, 128.8, 128.3, 128.2, 128.0, 127.6, 127.5, 127.5, 126.3, 107.9, 101.1, 80.2, 77.5, 76.7, 75.8, 75.6, 74.5, 73.6, 71.6, 69.9, 63.0, 49.6, 36.9, 31.9, 29.7, 29.5, 29.3, 29.2, 28.6, 26.9, 26.7, 25.8, 25.3, 22.7, 20.9, 14.1. **MS** (ESI): calcd for $C_{75}H_{121}NNaO_8^+$ $[M + Na]^+$, 1186.8990; found, 1186.8978.

*α-C-GC (**2**).* Compound **12** (24.6 mg, 0.021 mmol) was treated with 80% aqueous trifluoroacetic acid (20 mL) for 15 min and then concentrated. The mixture was co-evaporated three times with toluene (20 mL). The crude alcohol was used directly in the next reaction without any further purification. To a solution of the crude product from acidic hydrolysis in $CHCl_3$/MeOH (2:1, 30 mL) was added a palladium catalyst (10% Pd in charcoal, Pd/C, 50 mg) at rt. The mixture was stirred at rt for 4 h under an atmosphere of H_2. The suspension was filtered through a pressed pad of Celite which was prewashed with CH_2Cl_2/MeOH (1:1) to remove the inorganic salt, and the filtrate was concentrated under reduced pressure. The crude product was purified by flash column chromatography ($CHCl_3$/EtOH

https://doi.org/10.1021/acs.jmedchem.1c00881
J. Med. Chem. XXXX, XXX, XXX−XXX

= 2:1) on silica gel, which was prewashed with CH_2Cl_2/MeOH (1:1) to remove the inorganic salt, to provide **2** (9.04 mg, 50%). **^{1}H NMR** (600 MHz, d_5-pyridine): δ 8.59 (d, J = 8.7 Hz, 1H), 4.77 (s, 1H), 4.53 (s, 3H), 4.39 (s, 1H), 4.32−4.20 (m, 5H), 2.77 (s, 1H), 2.62 (s, 1H), 2.48 (s, 2H), 2.34 (d, J = 13.9 Hz, 2H), 2.22 (s, 1H), 1.96 (d, J = 14.6 Hz, 2H), 1.87 (t, J = 8.0 Hz, 2H), 1.72 (s, 1H), 1.37−1.13 (m, 74H), 0.87 (d, J = 7.4 Hz, 6H). **^{13}C NMR** (150 MHz, d_5-pyridine): δ 169.6, 146.5, 146.2, 146.0, 145.8, 132.0, 131.9, 131.7, 131.5, 131.3, 120.0, 119.8, 119.7, 119.5, 74.6, 73.2, 69.9, 68.7, 68.3, 66.7, 66.5, 58.9, 53.5, 48.7, 33.1, 30.6, 28.3, 26.5, 26.4, 26.2, 26.2, 26.1, 26.0, 26.0, 26.0, 25.8, 22.7, 22.5, 19.1, 18.7, 15.4, 10.4. **MS** (ESI): calcd for $C_{51}H_{101}NNaO_8^+$ $[M + Na]^+$, 878.74; found, 878.94.

*(2S,4aR,6S,7R,8S,8aS)-6-(Allyloxy)-7,8-bis(benzyloxy)-2-phenylhexahydropyrano[3,2-d][1,3]dioxine (**14**).* To a solution of compound **13** (273.9 mg, 0.64 mmol) and the activated 4 Å molecular sieves (600 mg) in dry DCM (40 mL) were added DMF (195.8 μL, 0.64 mmol), *N*-iodosuccinimide (142.6 mg, 0.64 mmol), and TMSOTf (7.5 μL, 0.95 mmol) at 0 °C, and the reaction mixture was stirred at 0 °C for 30 min. 3-Bromo-1-propanol (40.0 μL, 0.42 mmol) was then added dropwise, and the mixture was stirred at 0 °C for 3 h. The resulting mixture was filtered through a pressed pad of Celite, then the filtrate was quenched by the saturated $Na_2S_2O_3$ solution, and neutralized with $NaHCO_3$ aqueous solution. The biphasic mixture was separated, and the aqueous layers were extracted with CH_2Cl_2. The combined organic layers were dried (Na_2SO_4) and concentrated under reduced pressure. The resulting residue was purified by flash column chromatography on silica gel (petroleum ether/ethyl acetate = 85:15) to provide the glycosylation product. Then, to a solution of this product in *t*-BuOH (5 mL) at rt was added *t*-BuOK, and the solution was stirred at 90 °C for 3 h. To the mixture was added brine and extracted with EtOAc. The organic layer was dried (Na_2SO_4) and concentrated under reduced pressure to give compound **14** as a white solid (114.9 mg, 49% yield over two steps), which was not purified further by column chromatography. **^{1}H NMR** (400 MHz, $CDCl_3$): δ 7.63−7.47 (m, 2H), 7.33 (m, 13H), 5.91 (m, 1H), 5.47 (s, 1H), 5.31 (d, J = 17.2 Hz, 1H), 5.20 (d, J = 10.3 Hz, 1H), 4.97 (d, J = 3.4 Hz, 1H), 4.93−4.58 (m, 5H), 4.27−3.89 (m, 7H), 3.62 (s, 1H). **^{13}C NMR** (100 MHz, $CDCl_3$): δ 138.8, 138.5, 137.7, 133.7, 128.8, 128.2, 128.0, 127.9, 127.5, 127.4, 126.3, 118.0, 101.0, 96.8, 76.0, 75.4, 74.7, 73.5, 72.1, 69.3, 68.4, 62.6. **MS** (ESI): calcd for $C_{30}H_{32}NaO_6^+$ $[M + Na]^+$, 511.2097; found, 511.0278.

*(R,E)-1-(((2S,4aR,6S,7R,8S,8aS)-7,8-Bis(benzyloxy)-2-phenylhexahydropyrano[3,2-d][1,3]dioxin-6-yl)oxy)non-2-en-4-ol (**15-OCH**).* To a solution of compound **14** (977.6 mg, 2.00 mmol) and **7'** (511.0 mg, 3.00 mmol) in dry DCM (40 mL), Grubbs catalyst second generation (357.6 mg, 0.40 mmol) was added, giving rise to a brown solution, and the mixture was refluxed at 40 °C for 2 h. The solvent was removed under reduced pressure. The resulting residue was purified by flash column chromatography on silica gel (petroleum ether/ethyl acetate = 85:15) to provide the cross-metathesis product. Then, to a solution of this cross-metathesis product in DCM/MeOH (1:1, 30 mL) was added a 1.0 M NaOMe methanol solution (375.0 μL, 0.38 mmol), and the reaction mixture was stirred at rt for 3 h. Then, the solvent was removed under reduced pressure. The resulting residue was purified by flash column chromatography on silica gel (petroleum ether/ethyl acetate = 4:1) to provide **15-OCH** (410.6 mg, 41% yield over two steps). **^{1}H NMR** (600 MHz, $CDCl_3$) δ 7.59−7.21 (m, 15H), 5.76 (t, J = 4.3 Hz, 2H), 5.48 (s, 1H), 4.95 (d, J = 3.6 Hz, 1H), 4.93−4.58 (m, 4H), 4.29−3.95 (m, 8H), 3.64 (s, 1H), 1.54−1.20 (m, 8H), 0.89 (t, J = 6.6 Hz, 3H). **^{13}C NMR** (150 MHz, $CDCl_3$): δ 138.5, 138.4, 137.6, 136.7, 128.6, 128.0, 127.8, 127.6, 127.3, 127.3, 126.1, 125.4, 100.7, 96.6, 75.8, 75.2, 74.4, 73.3, 71.8, 71.7, 69.1, 67.2, 62.4, 36.8, 31.5, 24.8, 22.4, 13.8. **MS** (ESI): calcd for r $C_{36}H_{44}NaO_8^+$ $[M + Na]^+$, 627.2928; found, 627.3062.

*(R,E)-1-(((2S,4aR,6S,7R,8S,8aS)-7,8-Bis(benzyloxy)-2-phenylhexahydropyrano[3,2-d][1,3]dioxin-6-yl)oxy)octadec-2-en-4-ol (**15-αGC**).* This compound was prepared from **14** and **7** in 41% yield over two steps by the same procedure described above (**14** to **15-OCH**). **^{1}H NMR** (600 MHz, $CDCl_3$): δ 7.52 (d, J = 6.8 Hz, 2H), 7.35 (m, 13H), 5.48 (s, 1H), 4.95 (d, J = 3.4 Hz, 1H), 4.91−4.62 (m, 4H), 4.30−3.94 (m, 8H), 3.63 (s, 1H), 1.62 (s, 1H), 1.48 (t, J = 7.1 Hz, 2H), 1.26 (s, 22H), 0.88 (t, J = 6.6 Hz, 3H). **^{13}C NMR** (150 MHz, $CDCl_3$): δ 138.6, 137.9, 136.5, 128.8, 128.1, 127.5, 126.2,125.6, 100.9, 97.0, 76.1, 75.4, 74.6, 73.5, 72.0, 69.4, 67.4, 62.7, 37.1, 31.9, 25.3, 22.6, 14.0. **MS** (ESI): calcd for $C_{45}H_{62}NaO_7^+$ $[M + Na]^+$, 737.4393; found, 737.4389.

*(R)-1-((2R,3R)-3-((((2S,4aR,6S,7R,8S,8aS)-7,8-Bis(benzyloxy)-2-phenylhexahydropyrano[3,2-d][1,3]dioxin-6-yl)oxy)methyl)oxiran-2-yl)hexan-1-ol (**16-OCH**).* A solution of the activated 4 Å molecular sieves (317.8 mg), D-(−)-DIPT (101.5 μL, 0.48 mmol), and Ti(O-*i*Pr)$_4$ (118.9 μL, 0.40 mmol) in dry DCM (30 mL) at −40 °C was stirred for 1 h. **15-OCH** (235.6 mg, 0.40 mmol in 10 mL dry DCM) was added dropwise and the mixture was stirred at −40 °C for 30 min. Cumene hydroperoxide (139.1 μL, 0.80 mmol) was added and the mixture was stirred for another 36 h at −20 °C. Then, the mixture was filtered through a pressed pad of Celite, and the filtrate was quenched by 11% citric acid aqueous solution. The organic layer was dried (Na_2SO_4) and concentrated under reduced pressure. The resulting residue was purified by flash column chromatography on silica gel (petroleum ether/ethyl acetate = 4:1) to provide compound **16-OCH** (207.3 mg, 86%) as a white solid. **^{1}H NMR** (400 MHz, $CDCl_3$): δ 7.52 (d, J = 6.8 Hz, 2H), 7.44−7.24 (m, 13H), 5.48 (s, 1H), 4.96 (d, J = 3.3 Hz, 1H), 4.90−4.64 (m, 4H), 4.20 (m, 2H), 4.11−3.96 (m, 3H), 3.82 (d, J = 12.0 Hz, 1H), 3.78−3.71 (m, 1H), 3.68 (s, 1H), 3.55 (m, 1H), 3.28 (m, 1H), 2.96 (q, J = 2.3 Hz, 1H), 1.57−1.23 (m, 8H), 0.90 (t, J = 6.5 Hz, 3H). **^{13}C NMR** (150 MHz, $CDCl_3$): δ 138.7, 138.6, 137.7, 128.8, 128.3, 128.1, 127.9, 127.6, 127.5, 126.3, 101.0, 98.3, 75.8, 75.4, 74.6, 73.6, 72.1, 69.3, 68.3, 67.4, 62.7, 58.2, 53.2, 33.4, 31.8, 24.8, 22.5, 14.0. **MS** (ESI): calcd for $C_{36}H_{44}NaO_8^+$ $[M + Na]^+$, 627.2928; found, 627.3062.

*(R)-1-((2R,3R)-3-((((2S,4aR,6S,7R,8S,8aS)-7,8-Bis(benzyloxy)-2-phenylhexahydropyrano[3,2-d][1,3]dioxin-6-yl)oxy)methyl)oxiran-2-yl)pentadecan-1-ol (**16-αGC**).* This compound was prepared from **15-αGC** in 94% yield by the same procedure described above (**15-OCH** to **16-OCH**). **^{1}H NMR** (400 MHz, $CDCl_3$): δ 7.62−7.06 (m, 15H), 5.45 (s, 1H), 4.95 (d, J = 3.5 Hz, 1H), 4.91−4.61 (m, 4H), 4.25−3.89 (m, 6H), 3.79 (d, J = 12.2 Hz, 1H), 3.73−3.59 (m, 2H), 3.52 (m, 1H), 3.26 (d, J = 5.6 Hz, 1H), 2.92 (s, 1H), 1.43 (d, J = 10.1 Hz, 2H), 1.26 (s, 24H), 0.88 (t, J = 6.9 Hz, 3H). **^{13}C NMR** (150 MHz, $CDCl_3$): δ 138.6, 138.5, 137.7, 128.7, 128.2, 127.9, 127.8,127.6, 127.5, 127.4, 126.2, 100.8, 98.2, 75.7, 75.3, 74.4, 73.4, 71.9, 69.2, 68.2, 67.3, 62.5, 58.1, 53.1, 33.4, 31.8, 30.0, 29.5, 29.5, 29.2, 25.1, 22.5, 14.5, 14.0, 13.5. **MS** (ESI): calcd for $C_{45}H_{62}NaO_8^+$ $[M + Na]^+$, 753.4342; found, 753.4339.

*(2S,3S,4R)-2-Azido-1-(((2S,4aR,6S,7R,8S,8aS)-7,8-bis(benzyloxy)-2-phenylhexahydropyrano[3,2-d][1,3]dioxin-6-yl)oxy)nonane-3,4-diol (**17-OCH**).* A solution of compound **16-OCH** (205.0 mg, 0.34 mmol), NaN_3 (440.7 mg, 6.78 mmol), and NH_4Cl (181.3 mg, 3.39 mmol) in MeOH/H_2O (8:1, 9 mL) was heated in a sealed tube and stirred overnight at 100 °C. After cooling to rt, the mixture was treated with water and extracted with DCM. The organic layer was dried (Na_2SO_4) and concentrated under reduced pressure. The resulting residue was purified through flash column chromatography on silica gel (toluene/acetone = 30:1) to give compound **17-OCH** (92.2 mg, 42%) as a white solid. **^{1}H NMR** (600 MHz, CDCl3): δ 7.51 (d, J = 7.2 Hz, 2H), 7.42−7.23 (m, 13H), 5.47 (s, 1H), 4.95 (d, J = 11.6 Hz, 1H), 4.89−4.63 (m, 4H), 4.26−4.13 (m, 2H), 4.11−3.94 (m, 2H), 3.90−3.83 (m, 1H), 3.75 (s, 1H), 3.71 (s, 1H), 3.61 (s, 1H), 3.52 (s, 1H), 3.41 (s, 1H), 1.55 (d, J = 59.7 Hz, 2H), 1.29 (d, J = 22.6 Hz, 6H), 0.93−0.85 (m, 3H). **^{13}C NMR** (150 MHz, CDCl3): δ 138.3, 137.8, 137.7, 128.9, 128.5, 128.4, 128.3, 128.1, 128.1, 127.8, 127.7, 126.3, 101.1, 99.9, 76.4, 74.9, 74.7, 74.6, 74.1, 72.9, 71.9, 69.6, 69.3, 63.3, 59.7, 32.4, 31.8, 25.5, 22.6, 14.1. **MS** (ESI): calcd for $C_{36}H_{45}N_3NaO_8^+$ $[M + Na]^+$, 670.3099; found, 670.3090.

*(2S,3S,4R)-2-Azido-1-(((2S,4aR,6S,7R,8S,8aS)-7,8-bis(benzyloxy)-2-phenylhexahydropyrano[3,2-d][1,3]dioxin-6-yl)oxy)octadecane-3,4-diol (**17-αGC**).* This compound was prepared from **16-αGC** in 47% yield by the same procedure described above (**16-OCH** to **17-OCH**). **^{1}H NMR** (600 MHz, $CDCl_3$): δ 7.54 (d, J = 7.1 Hz, 2H), 7.37 (m, 13H), 5.50 (s, 1H), 4.97 (d, J = 11.7 Hz, 1H), 4.93−4.64 (m, 4H), 4.31−4.17 (m, 3H), 4.14−3.98 (m, 3H), 3.89 (m, 1H),

https://doi.org/10.1021/acs.jmedchem.1c00881
J. Med. Chem. XXXX, XXX, XXX−XXX

3.83−3.70 (m, 2H), 3.69−3.55 (m, 2H), 3.44 (m, 1H), 1.51 (m, 2H), 1.29 (m, 24H), 0.90 (t, J = 6.9 Hz, 3H). **^{13}C NMR** (150 MHz, $CDCl_3$): δ 138.2, 137.8, 137.6, 128.9, 128.5, 128.3, 128.3, 128.2, 128.1, 128.0, 127.8, 127.7, 126.2, 101.0, 99.8, 76.3, 74.8, 74.7, 74.5, 74.1, 72.8, 71.8, 69.6, 69.3, 63.2, 59.7, 32.4, 31.9, 29.7, 29.6, 29.3, 25.8, 22.7, 14.1. **MS** (ESI): calcd for $C_{45}H_{63}N_3NaO_8^+$ $[M + Na]^+$ 796.4513, found 796.4513.

*(2S,4aR,6S,7R,8S,8aS)-6-(((2S,3S,4R)-2-Azido-3,4-bis(benzyloxy)-nonyl)oxy)-7,8-bis(benzyloxy)-2-phenylhexahydropyrano[3,2-d]-[1,3]dioxine (**19-OCH**).* To a solution of compound **17-OCH** (55 mg, 0.085 mmol) in dry DMF (5 mL) was added NaH (8.2 mg, 0.34 mmol), and the solution was stirred at 0 °C for 15 min. Then, benzyl bromide (40 μL, 0.34 mmol) was added dropwise. The solution was stirred at 0 °C for 30 min. The reaction mixture was quenched with water and extracted with EtOAc. The combined organic layers were dried (Na_2SO_4) and concentrated under reduced pressure. The residue was purified by flash column chromatography on silica gel (petroleum ether/ethyl acetate = 20:1) to provide compound **19-OCH** (56.8 mg, 81%) as a white solid. **^{1}H NMR** (600 MHz, $CDCl_3$): δ 7.57−7.18 (m, 25H), 5.45 (s, 1H), 4.97 (d, J = 3.5 Hz, 1H), 4.88−4.47 (m, 8H), 4.22−3.97 (m, 5H), 3.87 (d, J = 12.5 Hz, 1H), 3.78−3.53 (m, 3H), 1.66 (m, 7.6 Hz, 1H), 1.53 (m, 1H), 1.47−1.38 (m, 1H), 1.27 (m, 5H), 0.88 (t, J = 7.1 Hz, 3H). **^{13}C NMR** (150 MHz, $CDCl_3$): δ 138.7, 138.3, 137.9, 137.8, 128.8, 128.3, 128.3, 128.2, 128.2, 128.1, 127.9, 127.8, 127.7, 127.7, 127.6, 127.6, 127.5, 127.4, 126.3, 101.0, 99.1, 79.4, 78.8, 73.7, 73.5, 72.0, 31.9, 22.6. **MS** (ESI): calcd for $C_{50}H_{57}N_3NaO_8^+$ $[M + Na]^+$, 850.4043; found, 850.4047.

*(2S,4aR,6S,7R,8S,8aS)-6-(((2S,3S,4R)-2-Azido-3,4-bis(benzyloxy)-octadecyl)oxy)-7,8-bis(benzyloxy)-2-phenylhexahydropyrano[3,2-d][1,3]dioxine (**19-αGC**).* This compound was prepared from **17-αGC** in 80% yield by the same procedure described above (**17-OCH** to **19-OCH**). **^{1}H NMR** (600 MHz, $CDCl_3$): δ 7.59−7.20 (m, 25H), 5.45 (s, 1H), 4.97 (d, J = 3.5 Hz, 1H), 4.90−4.45 (m, 8H), 4.25−3.50 (m, 11H), 1.66 (d, J = 11.1 Hz, 2H), 1.41 (s, 1H), 1.25 (d, J = 7.1 Hz, 23H), 0.88 (t, J = 6.9 Hz, 3H). **^{13}C NMR** (151 MHz, $CDCl_3$): δ 138.7, 138.3, 137.9, 137.7, 128.8, 128.3, 128.2,128.2, 128.1, 127.9, 127.8, 127.7, 127.5, 127.4, 126.3, 101.0, 99.1, 79.3, 78.8, 75.7, 75.4, 74.6, 73.7, 73.5, 72.0, 69.3, 68.4, 62.9, 61.7, 31.9, 31.6, 29.9, 29.7, 29.3, 25.4, 22.7, 14.1. **MS** (ESI): calcd for $C_{59}H_{75}N_3NaO_8^+$ $[M + Na]^+$, 976.5446; found, 976.5459.

*(2S,4aR,6S,7R,8S,8aS)-6-(((2S,3S,4R)-2-Azido-3,4-bis(benzyloxy)-nonyl)oxy)-7,8-bis(benzyloxy)-2-phenylhexahydropyrano[3,2-d]-[1,3]dioxine (**20-OCH**).* PMe_3 (0.5 mL, 0.50 mmol) was added to a solution of **19-OCH** (112.6 mg, 0.14 mmol) in wet MeOH (2 mL) at rt, and the resulting solution was stirred for 2 h. Then, the reaction mixture was concentrated under reduced pressure. The residue was then subjected to high vacuum at rt for 3 h. The crude amine was used in the next step without further purification. To the solution of the crude amine in a mixture solvent CH_2Cl_2/MeOH (2:1, 3 mL) was added Et_3N (0.5 mL) followed by the solution of the freshly prepared *n*-hexacosanoyl acid chloride (0.408 mmol in 2 mL CH_2Cl_2) at rt. The mixture was stirred at rt for 30 min, quenched with saturated aqueous NH_4Cl solution, and extracted with CH_2Cl_2 (3 × 30 mL). The combined organic layers were dried (Na_2SO_4), concentrated, and purified by flash chromatography (petroleum ether/ethyl acetate = 3:1) to give **20-OCH** (97.9 mg, 61% over two steps). **^{1}H NMR** (600 MHz, $CDCl_3$): δ 7.77−7.16 (m, 30H), 5.78 (d, J = 8.2 Hz, 1H), 5.45 (s, 1H), 4.94 (d, J = 3.6 Hz, 1H), 4.85 (d, J = 11.7 Hz, 1H), 4.73 (m, 3H), 4.61 (m, 2H), 4.54−4.43 (m, 2H), 4.30 (q, J = 7.9, 7.4 Hz, 2H), 4.17 (d, J = 3.2 Hz, 1H), 4.12−4.01 (m, 2H), 3.92 (t, J = 13.5 Hz, 3H), 3.82−3.72 (m, 2H), 3.58 (s, 1H), 1.94−1.81 (m, 1H), 1.77−1.54 (m, 5H), 1.45 (m, 5H), 1.25 (d, J = 7.3 Hz, 86H), 0.87 (q, J = 7.3 Hz, 6H). **^{13}C NMR** (150 MHz, $CDCl_3$): δ 172.9, 138.6, 138.5, 138.4, 137.8, 130.9, 128.8, 128.4, 128.4, 128.3, 128.1, 127.9, 127.8, 127.7, 127.6, 127.6, 127.5, 126.3, 101.0, 99.7, 79.8, 79.4, 76.1, 75.6, 74.3, 73.8, 73.3, 71.9, 71.7, 69.4, 68.2, 65.5, 62.9, 50.3, 36.7, 31.9, 30.5, 30.2, 29.7, 29.7, 29.6, 29.4, 29.4, 25.7, 25.5, 22.7, 22.6, 19.2, 14.1, 14.1, 13.7. **MS** (ESI): calcd for $C_{76}H_{109}NNaO_9^+$ $[M + Na]^+$, 1202.8000; found, 1202.7972.

*(2S,4aR,6S,7R,8S,8aS)-6-(((2S,3S,4R)-2-Azido-3,4-bis(benzyloxy)-octadecyl)oxy)-7,8-bis(benzyloxy)-2-phenylhexahydropyrano[3,2-d][1,3]dioxine (**20-αGC**).* This compound was prepared from **19-αGC** in 81% yield by the procedure described above (**19-OCH** to **20-OCH**). **^{1}H NMR** (600 MHz, $CDCl_3$): δ 7.62−7.16 (m, 25H), 5.79 (d, J = 8.2 Hz, 1H), 5.48 (s, 1H), 4.96 (d, J = 3.5 Hz, 1H), 4.91−4.46 (m, 8H), 4.37−3.46 (m, 11H), 1.89 (m, 2H), 1.73−1.59 (m, 3H), 1.55−1.43 (m, 2H), 1.46−1.09 (m, 67H), 0.90 (t, J = 6.9 Hz, 6H). **^{13}C NMR** (151 MHz, $CDCl_3$): δ 172.9, 138.5, 128.8, 128.4, 128.4, 128.3, 128.3, 128.1, 127.9, 127.8, 127.7, 127.6, 127.5, 126.3, 101.0, 99.7, 79.8, 76.9, 75.7, 74.4, 73.8, 71.9, 69.4, 62.9, 36.7, 31.9, 29.7, 29.7, 29.6, 29.5, 29.4, 25.7, 22.7, 14.1. **MS** (ESI): calcd for $C_{85}H_{127}NNaO_9^+$ $[M + Na]^+$, 1328.9403; found, 1329.0713.

*OCH (**3**).* To a solution of **20-OCH** (34.3 mg, 0.029 mmol) in $CHCl_3$/MeOH (2:1, 6 mL) was added, at rt, a palladium catalyst (10% Pd in charcoal, Pd/C, 50 mg). The mixture was stirred at rt for 4 h under an atmosphere of H_2. The suspension was filtered through a pressed pad of Celite, which was prewashed with $CHCl_3$/MeOH (1:1) to remove the inorganic salt, and the filtrate was concentrated under reduced pressure. The resulting crude product was purified by flash column chromatography ($CHCl_3$/MeOH = 7:1) to yield the product OCH (14.5 mg, 68%). **^{1}H NMR** (600 MHz, $CD_3OD/CDCl_3$ = 1:1): δ 4.91 (d, J = 2.9 Hz, 1H), 4.21 (s, 1H), 4.16 (s, 1H), 3.93 (s, 1H), 3.89 (s, 1H), 3.75 (m, 6H), 3.55 (s, 2H), 2.21 (d, J = 8.2 Hz, 2H), 1.65 (d, J = 41.1 Hz, 2H), 1.27 (m, 52H), 0.91−0.87 (m, 6H). **^{13}C NMR** (150 MHz, $CD_3OD/CDCl_3$ = 1:1): δ 175.3, 100.5, 75.2, 72.5, 71.7, 70.9, 70.4, 69.6, 67.8, 62.4, 51.1, 37.0, 32.9, 32.5, 30.3, 30.3, 30.2, 30.0, 30.0, 26.6, 26.1, 23.3, 14.3. **MS** (ESI): calcd for $C_{41}H_{82}NO_9^+$ $[M + H]^+$, 732.5984; found, 732.6138.

*αGC (**1**).* This compound was prepared from **20-αGC** in 68% yield by the same procedure described above (**20-OCH** to **OCH**). **^{1}H NMR** (600 MHz, d_5-pyridine): δ 8.56 (d, J = 8.6 Hz, 1H), 5.60 (d, J = 3.9 Hz, 1H), 5.30 (d, J = 9.3 Hz, 1H), 4.69 (m, 2H), 4.63−4.50 (m, 2H), 4.43 (m, 4H), 4.35 (s, 2H), 2.46 (t, J = 7.5 Hz, 2H), 1.98−1.66 (m, 7H), 1.48−1.14 (m, 71H), 0.88 (t, J = 6.8 Hz, 6H). **^{13}C NMR** (150 MHz, d_5-pyridine): δ 173.0, 101.2, 76.4, 72.8, 72.2, 71.4, 70.7, 70.0, 68.4, 62.4, 51.2, 36.5, 34.1, 31.9, 30.1, 29.8, 29.4, 26.2, 22.7, 14.0. **MS** (ESI) calcd for $C_{50}H_{99}NNaO_9^+$ $[M + Na]^+$, 880.72; found, 880.92.

*C20:2 (**4**).* PMe_3 (1.75 mL, 1.75 mmol) was added to a solution of **21** (300 mg, 0.35 mmol) in MeOH (20 mL) at rt, and the resulting solution was stirred for 3 h. Then, the solvent was concentrated under reduced pressure. The crude amine was used in the next step without further purification. To a solution of crude amine (20 mg) in EtOH/MeOH (3:1, 20 mL) was added a palladium catalyst [$Pd(OH)_2$ in charcoal, $Pd(OH)_2$/C, 10 mg] at rt; the reaction vessel was purged with H_2 for 10 min. The mixture was stirred at rt for 4 h under H_2. The suspension was filtered through a pressed pad of Celite, which was prewashed with $CHCl_3$/EtOH (1:1), and the filtrate was concentrated under reduced pressure to give compound **22**. To the solution of amine **22** (10 mg, 0.02 mmol) in a mixture solvent CH_2Cl_2/MeOH (2:1, 3 mL) was added Et_3N (0.5 mL) followed by the solution of the freshly prepared chloride **23** (0.060 mmol, in 2 mL CH_2Cl_2) at 0 °C. The mixture was stirred at rt for 10 min, quenched with saturated aqueous NH_4Cl solution, and extracted with CH_2Cl_2 (3 × 30 mL). The combined organic layers were dried (Na_2SO_4), concentrated, and purified by flash column chromatography (CH_2Cl_2/MeOH = 9:1) to yield C20:2 (**4**, 10 mg, 65%) as a white solid. **^{1}H NMR** (400 MHz, $CD_3OD/CDCl_3$ = 1:1): δ 5.35 (d, J = 5.9 Hz, 3H), 4.91 (d, J = 3.7 Hz, 1H), 4.35 (s, 15H), 3.94 (d, J = 2.8 Hz, 1H), 3.88 (m, 1H), 3.79 (s, 2H), 3.74 (d, J = 4.0 Hz, 1H), 3.71 (d, J = 5.5 Hz, 1H), 3.68 (s, 1H), 3.55 (d, J = 5.3 Hz, 1H), 3.43−3.30 (m, 2H), 3.17 (m, 3H), 2.78 (t, J = 6.4 Hz, 2H), 2.28−2.14 (m, 2H), 2.12−1.99 (m, 3H), 1.63 (s, 4H), 1.45−1.10 (m, 34H), 0.88 (t, J = 5.9 Hz, 6H). **^{13}C NMR** (100 MHz, $CD_3OD/CDCl_3$ = 1:1): δ 174.8, 130.4, 130.4, 128.2, 128.2, 100.0, 78.5, 75.0, 72.3, 71.1, 70.6, 70.0, 69.2, 67.2, 62.1, 50.7, 36.3, 32.2, 31.8, 31.0, 30.0, 29.9, 29.9, 29.8, 29.7, 29.7, 29.6, 27.5, 27.4, 26.2, 25.9, 22.9, 22.8, 13.2. **MS** (ESI) calculated for $C_{44}H_{83}NNaO_9^+$ $[M + Na]^+$, 792.60; found, 792.74.

https://doi.org/10.1021/acs.jmedchem.1c00881
J. Med. Chem. XXXX, XXX, XXX−XXX

*Dioxolane **25** and Dioxane **26**.* To a solution of compound **17-OCH** (64.3 mg, 0.099 mmol) in anhydrous DCM (5 mL) were added PPTS (2.5 mg, 0.010 mmol) and 2,2-DMP (124.5 μL, 0.992 mmol), and the solution was stirred at rt overnight. The mixture was concentrated under reduced pressure. The resulting residue was purified through flash column chromatography on silica gel (petroleum ether/ethyl acetate = 9:1) to provide compound **25** (50.5 mg, 74%) as a white solid. Compound **26** was synthesized using the same method from **18-OCH** (72%). NMR data for **25**: **^{1}H NMR** (600 MHz, $CDCl_3$): δ 7.52 (d, J = 7.2 Hz, 2H), 7.34 (m, 13H), 5.48 (s, 1H), 5.03 (d, J = 3.3 Hz, 1H), 4.77 (m, 4H), 4.27−4.15 (m, 2H), 4.15−3.98 (m, 6H), 3.77 (m, 1H), 3.68 (s, 1H), 3.38 (t, J = 7.4 Hz, 1H), 1.65−1.46 (m, 2H), 1.45−1.24 (m, 12H), 0.91 (d, J = 6.6 Hz, 3H). **^{13}C NMR** (150 MHz, $CDCl_3$): δ 138.9, 138.8, 137.8, 128.9, 128.2, 128.2, 128.1, 127.7, 127.6, 127.5, 127.4, 126.3, 108.2, 101.1, 99.4, 77.7, 75.6, 75.0, 74.9, 73.2, 72.3, 69.5, 69.4, 63.1, 59.7, 31.8, 29.3, 28.2, 26.1, 25.7, 22.6, 14.0. **26**: **^{1}H NMR** (600 MHz, $CDCl_3$): δ 7.52 (d, J = 6.9 Hz, 2H), 7.46−7.24 (m, 10H), 5.49 (s, 1H), 5.09 (d, J = 3.6 Hz, 1H), 4.79 (m, 4H), 4.27−4.16 (m, 2H), 4.13−3.97 (m, 3H), 3.75 (m, 5H), 3.43 (m, 1H), 1.66−1.55 (m, 2H), 1.48−1.12 (m, 12H), 0.90 (t, J = 6.7 Hz, 3H). **^{13}C NMR** (150 MHz, $CDCl_3$): δ 138.7, 137.8, 128.8, 128.3, 128.2, 128.1, 127.7, 127.5, 127.5, 126.3, 101.1, 101.0, 98.2, 75.6, 75.4, 74.7, 73.2, 72.1, 71.5, 70.3, 69.4, 67.6, 62.8, 62.6, 31.7, 29.9, 25.3, 24.4, 23.9, 22.5, 14.0.

Immunological Test. *Materials and Reagents.* DSPC was purchased from TCI. Cholesterol was purchased from Energy Chemical. Peroxidase-conjugated AffiniPure goat anti-mouse kappa, IgA, IgE, IgG1, IgG2a, IgG2b, and IgG3 antibodies were purchased from Southern Biotechnology, peroxidase-conjugated AffiniPure goat anti-mouse κ antibodies IgG and IgM were purchased from Jackson Immuno Research. RBD-Fc (catalogue number: 40592-V02H), and RBD-His (catalogue number: 40592-V08B) proteins were purchased from Sino Biological, Beijing, China (see the Supporting Information for the details). The Alum adjuvant (Imject Alum) was purchased from Thermo Scientific, which contains an aqueous solution of aluminum hydroxide and magnesium hydroxide plus inactive stabilizers.

Vaccine Formulations. Liposomal formulations of these vaccine candidates were prepared according to our previous reports[53,65] with a slight modification. The composition of each vaccine candidate is shown in Tables S2 and S3 in the Supporting Information. The procedures for liposomal formulation are as follows: the glycolipid (αGC, α-C-GC, OCH, C20:2), DSPC, and cholesterol (in a molar ratio of 1:4.79:2.05) were dissolved in DCM/MeOH (1:1, v/v, 2 mL), and the solvents were removed under reduced pressure through rotary evaporation, which generated a thin lipid film on the flask wall. This film was hydrated and subjected to freeze/thaw cycles to produce multilamellar vesicles, to which PBS buffer (20 mM, pH 7.5) was added and left to stand for 0.5 h, then the mixture was shaken under an argon atmosphere at rt for 1 h, and the RBD-Fc protein was added. After shaking for 0.5 h, the suspension was used immediately. The solution forms were prepared by dissolving the glycolipid (αGC, α-C-GC, OCH, C20:2) in DMSO (1% volume of PBS buffer), followed by the addition of PBS buffer and shaking the mixture under an argon atmosphere at rt for 1 h, and then the addition of RBD-Fc. After shaking for 0.5 h, the solution was used immediately. Vaccine candidates using Alum adjuvants were prepared, according to manufacturer's instructions, by mixing the RBD-Fc solution in PBS buffer with an equal volume of the Alum adjuvant solution, then shaking at rt for 1 h before immunization.

Immunization of Mice. The animal experiments were conducted according to the animal ethics guidelines (Regulations of Hubei Province on the Administration of Experimental Animals and Measures of Hubei Province on the Administration of Laboratory Animal Licenses) and were approved by the Scientific Ethics Committee of Huazhong Agricultural University. Specific pathogen-free female 6−8 week old BALB/c mice were purchased from the Laboratory Animal Center of Huazhong Agriculture University. All mice used in this study are in good health. Upon arrival, mice were housed with five companions per cage and fed for a week. All animals were allowed free access to water and standard chow diets and provided with a 12 h light and dark cycle (temperature: 22−25 °C; humidity: 60−70%). Groups of five female BALB/c mice were bred in the Laboratory Animal Center of Huazhong Agriculture University. The mice were subcutaneously immunized with the vaccine candidates (see Tables S2 and S3 for the detailed composition) on day 1, day 15, and day 29. The mice were bled on day 0 before initial immunization and day 14, day 28, and day 42. The mouse blood samples were clotted to obtain antisera that were stored at −30 °C before use.

RBD-Specific Antibody Determined by ELISA. A 96-well microtiter plate (Costar type 3590, Corning Inc.) was first coated with 10 μg of RBD-His (Sino Biological), which had been dissolved in 0.1 M bicarbonate buffer (pH = 9.6). The plate was then incubated at 4 °C overnight. The plate was then washed three times with PBST (0.05% Tween-20 in PBS), followed by the addition of 200 μL of 3% (w/v) BSA in PBS to each well and incubation at 37 °C for 1 h. After the plate was washed again with PBST, serially diluted sera were added to microwells (100 μL/well) and incubated for 1 h 40 min at 37 °C and washed (three times). A 1:5000 diluted solution of horseradish peroxidase (HRP)-conjugated goat anti-mouse IgM or IgG or IgG subtype (IgG1, IgG2a, IgG2b, and IgG3) in PBST (100 μL per well) was added to each well, respectively. The plate was incubated for 1 h at 37 °C. After a final wash (five times), substrate solutions that were freshly prepared with 9.5 mL of critic buffer at pH 5.0, 0.5 mL of 2 mg/mL tetramethyl benzidine, and 32 μL of 3% (w/v) urea hydrogen peroxide were added to the wells (100 μL per well). The color was allowed to develop in the dark for 5 min and then a solution of 2 M H_2SO_4 was added to quench the reaction. The optical density was then measured at 450 nm. The antibody titer was defined as the highest dilution showing an absorbance of 0.1, after subtracting the background. Pre-immunization sera were used as a negative control.

Cells and Plasmids. HEK293T cells were purchased from ATCC and cultured in Dulbecco's Modified Eagle's Medium (DMEM, Gibco) supplemented with 10% fetal bovine serum (FBS, Gibco), 100 mg/mL of streptomycin, and 100 unit/mL of penicillin at 37 °C in 5% CO_2. HeLa cells expressing ACE2 were cultured in DMEM with 10% FBS and 0.2 mg/mL hygromycin. The plasmid pCDNA3.1-SARS-CoV-2-S was kindly provided by Prof. Xingyi Ge (Hunan University, China). The lentiviral packaging plasmid psPAX2 and the pLenti-GFP reporter plasmid expressing both GFP and firefly luciferase were purchased from Addgene (Cambridge, MA).

SARS-CoV-2 Pseudovirus Production and Titration. For the preparation of the SARS-CoV-2 pseudovirus, psPAX2, pLenti-GFP, and pCDNA3.1-SARS-CoV-2-S were co-transfected into HEK293T cells at a 1:1:1 ratio. 48 h after transfection, the cell supernatant was collected, centrifuged at 800 g for 15 min, followed by filtration through 0.45 μm filters to remove cell debris, and the viral stocks were aliquoted and preserved at −80 °C until use. The viral stock was titrated in HeLa-ACE2 cells. Briefly, HeLa-ACE2 cells were seeded into 96-well plates and incubated with 50 μL of media containing pseudovirions. After 8 h incubation, the supernatant was replaced with fresh DMEM containing 2% FBS. At 48 h, postincubation, the cells were lysed with 30 μL of lysis buffer (Promega, Madison, WI, USA), and the transduction efficiency was measured by the quantification of the luciferase activity using the Luciferase Assay Kit (Promega) according to the manufacturer's instructions. All the experiments were done in triplicates and repeated at least twice.

SARS-CoV-2 Pseudovirus Neutralization Assay. Neutralizing antibodies in mice were assessed by the SARS-CoV-2-pseudo-typed neutralization assay as described previously.[75] HeLa-ACE2 cells were plated into 96-well plates at 5000 cells/well 1 day before the experiment. The collected serum was heated for 30 min at 56 °C to inactivate the complement. The serial 2-fold dilutions of sera (with an initial dilution of 1:100) or serial 3-fold dilutions of sera (with an initial dilution of 1:10) were incubated for 1 h at 37 °C with an equal volume of the SARS-CoV-2 pseudovirus. Subsequently, the serum virus mix was added to the HeLa-ACE2 cells. After 48 h, the cells were lysed, and the luciferase activity was measured using a Firefly Luciferase Assay Kit (Promega, Madison, WI, USA). Neutralization

https://doi.org/10.1021/acs.jmedchem.1c00881
J. Med. Chem. XXXX, XXX, XXX−XXX

titers (IC_{50}) were calculated as the reciprocal of the serum dilution that resulted in a 50% reduction in RLUs compared to virus control wells after the subtraction of background RLU. The 1:100 serum dilution was the limit of quantitation in this assay. Serum samples that did not exhibit neutralizing activities or that neutralized at levels higher than 1:100 were calculated as the limit of the quantitation for statistical analyses. IC_{50} below the limit of detection was determined as half the limit of detection.

Statistical Analysis. Data reported in the figures were analyzed using Prism 6 (GraphPad Software). All values and error bars are mean ± SEM. The significance between the two groups was determined by the unpaired two-tailed Student's t-test. The significance of multiple groups in comparison to the control group was evaluated using one-way ANOVA followed by Dunnett's multiple comparison test. Asterisks (*, $P \leq 0.05$; **, $P \leq 0.01$; ***, $P \leq 0.001$; ****, $P \leq 0.001$; ns, not significant) indicate significant differences.

■ ASSOCIATED CONTENT

Supporting Information

The Supporting Information is available free of charge at https://pubs.acs.org/doi/10.1021/acs.jmedchem.1c00881.

Compound characterization spectra (HPLC-ELSD, ^1H NMR, and ^{13}C NMR), vaccine liposomal formulations, information of RBD-Fc and RBD-His, and biological assays (IgM, IgG subtype response induced by a different dose of RBD-Fc) (PDF)

Molecular formula strings of the compounds (CSV)

■ AUTHOR INFORMATION

Corresponding Authors

Rui Luo − *State Key Laboratory of Agricultural Microbiology, College of Veterinary Medicine, Huazhong Agricultural University, Wuhan, Hubei 430070, P. R. China*; Email: luorui@mail.hzau.edu.cn

Zheng Liu − *Key Laboratory of Pesticide & Chemical Biology of Ministry of Education, Hubei International Scientific and Technological Cooperation Base of Pesticide and Green Synthesis, International Joint Research Center for Intelligent Biosensing Technology and Health, College of Chemistry, Central China Normal University, Wuhan, Hubei 430079, P. R. China*; orcid.org/0000-0002-3696-339X; Email: liuz1118@mail.ccnu.edu.cn

Authors

Xi-Feng Wang − *Key Laboratory of Pesticide & Chemical Biology of Ministry of Education, Hubei International Scientific and Technological Cooperation Base of Pesticide and Green Synthesis, International Joint Research Center for Intelligent Biosensing Technology and Health, College of Chemistry, Central China Normal University, Wuhan, Hubei 430079, P. R. China*

Meng-Jia Zhang − *State Key Laboratory of Agricultural Microbiology, College of Veterinary Medicine, Huazhong Agricultural University, Wuhan, Hubei 430070, P. R. China*

Na He − *Key Laboratory of Pesticide & Chemical Biology of Ministry of Education, Hubei International Scientific and Technological Cooperation Base of Pesticide and Green Synthesis, International Joint Research Center for Intelligent Biosensing Technology and Health, College of Chemistry, Central China Normal University, Wuhan, Hubei 430079, P. R. China*

Ya-Cong Wang − *Key Laboratory of Pesticide & Chemical Biology of Ministry of Education, Hubei International Scientific and Technological Cooperation Base of Pesticide and Green Synthesis, International Joint Research Center for Intelligent Biosensing Technology and Health, College of Chemistry, Central China Normal University, Wuhan, Hubei 430079, P. R. China*

Cheng Yan − *Key Laboratory of Pesticide & Chemical Biology of Ministry of Education, Hubei International Scientific and Technological Cooperation Base of Pesticide and Green Synthesis, International Joint Research Center for Intelligent Biosensing Technology and Health, College of Chemistry, Central China Normal University, Wuhan, Hubei 430079, P. R. China*

Xiang-Zhao Chen − *Key Laboratory of Prevention and Treatment of Cardiovascular and Cerebrovascular Diseases of Ministry of Education, Gannan Medical University, Ganzhou, Jiangxi 341000, China*

Xiao-Fei Gao − *Jiangxi Key Laboratory for Mass Spectrometry and Instrumentation, East China University of Technology, Nanchang, Jiangxi 330013, China*

Jun Guo − *Key Laboratory of Pesticide & Chemical Biology of Ministry of Education, Hubei International Scientific and Technological Cooperation Base of Pesticide and Green Synthesis, International Joint Research Center for Intelligent Biosensing Technology and Health, College of Chemistry, Central China Normal University, Wuhan, Hubei 430079, P. R. China*; orcid.org/0000-0002-2097-5054

Complete contact information is available at: https://pubs.acs.org/10.1021/acs.jmedchem.1c00881

Author Contributions

⊥X.-F.W. and M.-J.Z. contributed equally.

Funding

This work was supported by the National Natural Science Foundation of China (nos. 21977034 and 21772056), Wuhan Bureau of Science and Technology (2018060401011323), self-determined research funds of CCNU from the Colleges' Basic Research and Operation of MOE (nos. CCNU20TS016 and CCNU20TS014), Fundamental Research Funds for the Central Universities (grant no. 2662019PY078), Open Project of Key Laboratory of Prevention and Treatment of Cardiovascular and Cerebrovascular Diseases, Ministry of Education (XN202006), Research Fund of East China University of Technology (no. DHBK2017114), and Program of Introducing Talents of Discipline to Universities of China (111 Program, B17019).

Notes

The authors declare no competing financial interest.

■ ABBREVIATIONS

αGC, α-galactosylceramide; ACE2, angiotensin-converting enzyme 2; APC, antigen-presenting cells; 9-BBN, 9-borabicyclo[3.3.1]nonane; BSA, bovine serum albumin; DCs, dendritic cells; DCM, dichloromethane; DIPEA, *N*,*N*-diisopropylethylamine; 2,2-DMP, 2,2-dimethoxypropane; DMEM, Dulbecco's modified Eagle's medium; DSPC, 1,2-distearoyl-*sn*-glycero-3-phosphocholine; ELISA, enzyme-linked immunosorbent assay; ELSD, evaporative light scattering detector; ESI, electrospray ionization; FBS, fetal bovine serum; HRP, horseradish peroxidase; IC_{50}, half-maximal inhibitory concentration; IFN-γ, interferon-γ; IL-4, interleukin-4; iNKT, invariant natural killer T; MHC, major histocompatibility complex; MTPA, methoxy-α-(trifluoromethyl)phenylacetic acid; PPTS, pyridinium 4-

toluenesulfonate; RBD, receptor-binding domain; SARS-CoV-2, severe acute respiratory syndrome coronavirus 2; TLC, thin-layer chromatography

REFERENCES

(1) Rappuoli, R.; De Gregorio, E.; Del Giudice, G.; Phogat, S.; Pecetta, S.; Pizza, M.; Hanon, E. Vaccinology in the Post−COVID-19 Era. *Proc. Natl. Acad. Sci. U.S.A.* **2021**, *118*, No. e2020368118.

(2) Pollard, A. J.; Bijker, E. M. A Guide to Vaccinology: From Basic Principles to New Developments. *Nat. Rev. Immunol.* **2021**, *21*, 83−100.

(3) Grant, O. C.; Montgomery, D.; Ito, K.; Woods, R. J. Analysis of the SARS-CoV-2 Spike Protein Glycan Shield Reveals Implications for Immune Recognition. *Sci. Rep.* **2020**, *10*, 14991.

(4) Sun, S.; He, L.; Zhao, Z.; Gu, H.; Fang, X.; Wang, T.; Yang, X.; Chen, S.; Deng, Y.; Li, J.; Zhao, J.; Li, L.; Li, X.; He, P.; Li, G.; Li, H.; Zhao, Y.; Gao, C.; Lang, X.; Wang, X.; Fei, G.; Li, Y.; Geng, S.; Gao, Y.; Wei, W.; Hu, Z.; Han, G.; Sun, Y. Recombinant Vaccine Containing an RBD-Fc Fusion Induced Protection against SARS-CoV-2 in Nonhuman Primates and Mice. *Cell. Mol. Immunol.* **2021**, *18*, 1070−1073.

(5) Ye, F.; Zhao, J.; Xu, P.; Liu, X.; Yu, J.; Shangguan, W.; Liu, J.; Luo, X.; Li, C.; Ying, T.; Wang, J.; Yu, B.; Wang, P. Synthetic Homogeneous Glycoforms of the SARS-CoV-2 Spike Receptor-Binding Domain Reveals Different Binding Profiles of Monoclonal Antibodies. *Angew. Chem., Int. Ed.* **2021**, *60*, 12904−12910.

(6) Dai, L.; Zheng, T.; Xu, K.; Han, Y.; Xu, L.; Huang, E.; An, Y.; Cheng, Y.; Li, S.; Liu, M.; Yang, M.; Li, Y.; Cheng, H.; Yuan, Y.; Zhang, W.; Ke, C.; Wong, G.; Qi, J.; Qin, C.; Yan, J.; Gao, G. F. A Universal Design of Betacoronavirus Vaccines against COVID-19, MERS, and SARS. *Cell* **2020**, *182*, 722−733.

(7) Walls, A. C.; Fiala, B.; Schäfer, A.; Wrenn, S.; Pham, M. N.; Murphy, M.; Tse, L. V.; Shehata, L.; O'Connor, M. A.; Chen, C.; Navarro, M. J.; Miranda, M. C.; Pettie, D.; Ravichandran, R.; Kraft, J. C.; Ogohara, C.; Palser, A.; Chalk, S.; Lee, E.-C.; Guerriero, K.; Kepl, E.; Chow, C. M.; Sydeman, C.; Hodge, E. A.; Brown, B.; Fuller, J. T.; Dinnon, K. H.; Gralinski, L. E.; Leist, S. R.; Gully, K. L.; Lewis, T. B.; Guttman, M.; Chu, H. Y.; Lee, K. K.; Fuller, D. H.; Baric, R. S.; Kellam, P.; Carter, L.; Pepper, M.; Sheahan, T. P.; Veesler, D.; King, N. P. Elicitation of Potent Neutralizing Antibody Responses by Designed Protein Nanoparticle Vaccines for SARS-CoV-2. *Cell* **2020**, *183*, 1367−1382.e17.

(8) Dai, L.; Gao, G. F. Viral Targets for Vaccines against COVID-19. *Nat. Rev. Immunol.* **2021**, *21*, 73−82.

(9) Zhao, Q.; Gao, Y.; Xiao, M.; Huang, X.; Wu, X. Synthesis and Immunological Evaluation of Synthetic Peptide Based Anti-SARS-CoV-2 Vaccine Candidates. *Chem. Commun.* **2021**, *57*, 1474−1477.

(10) Yang, J.; Wang, W.; Chen, Z.; Lu, S.; Yang, F.; Bi, Z.; Bao, L.; Mo, F.; Li, X.; Huang, Y.; Hong, W.; Yang, Y.; Zhao, Y.; Ye, F.; Lin, S.; Deng, W.; Chen, H.; Lei, H.; Zhang, Z.; Luo, M.; Gao, H.; Zheng, Y.; Gong, Y.; Jiang, X.; Xu, Y.; Lv, Q.; Li, D.; Wang, M.; Li, F.; Wang, S.; Wang, G.; Yu, P.; Qu, Y.; Yang, L.; Deng, H.; Tong, A.; Li, J.; Wang, Z.; Yang, J.; Shen, G.; Zhao, Z.; Li, Y.; Luo, J.; Liu, H.; Yu, W.; Yang, M.; Xu, J.; Wang, J.; Li, H.; Wang, H.; Kuang, D.; Lin, P.; Hu, Z.; Guo, W.; Cheng, W.; He, Y.; Song, X.; Chen, C.; Xue, Z.; Yao, S.; Chen, L.; Ma, X.; Chen, S.; Gou, M.; Huang, W.; Wang, Y.; Fan, C.; Tian, Z.; Shi, M.; Wang, F.-S.; Dai, L.; Wu, M.; Li, G.; Wang, G.; Peng, Y.; Qian, Z.; Huang, C.; Lau, J. Y.-N.; Yang, Z.; Wei, Y.; Cen, X.; Peng, X.; Qin, C.; Zhang, K.; Lu, G.; Wei, X. A Vaccine Targeting the RBD of the S Protein of SARS-CoV-2 Induces Protective Immunity. *Nature* **2020**, *586*, 572−577.

(11) Levin, D.; Golding, B.; Strome, S. E.; Sauna, Z. E. Fc Fusion as a Platform Technology: Potential for Modulating Immunogenicity. *Trends Biotechnol.* **2015**, *33*, 27−34.

(12) Qi, X.; Ke, B.; Feng, Q.; Yang, D.; Lian, Q.; Li, Z.; Lu, L.; Ke, C.; Liu, Z.; Liao, G. Construction and Immunogenic Studies of a mFc Fusion Receptor Binding Domain (RBD) of Spike Protein as a Subunit Vaccine against SARS-CoV-2 Infection. *Chem. Commun.* **2020**, *56*, 8683−8686.

(13) Liu, X.; Drelich, A.; Li, W.; Chen, C.; Sun, Z.; Shi, M.; Adams, C.; Mellors, J. W.; Tseng, C.-T.; Dimitrov, D. S. Enhanced Elicitation of Potent Neutralizing Antibodies by the SARS-CoV-2 Spike Receptor Binding Domain Fc Fusion Protein in Mice. *Vaccine* **2020**, *38*, 7205−7212.

(14) Liu, Z.; Xu, W.; Xia, S.; Gu, C.; Wang, X.; Wang, Q.; Zhou, J.; Wu, Y.; Cai, X.; Qu, D.; Ying, T.; Xie, Y.; Lu, L.; Yuan, Z.; Jiang, S. RBD-Fc-Based COVID-19 Vaccine Candidate Induces Highly Potent SARS-CoV-2 Neutralizing Antibody Response. *Signal Transduction Targeted Ther.* **2020**, *5*, 282.

(15) Gu, H.; Chen, Q.; Yang, G.; He, L.; Fan, H.; Deng, Y.-Q.; Wang, Y.; Teng, Y.; Zhao, Z.; Cui, Y.; Li, Y.; Li, X.-F.; Li, J.; Zhang, N.-N.; Yang, X.; Chen, S.; Guo, Y.; Zhao, G.; Wang, X.; Luo, D.-Y.; Wang, H.; Yang, X.; Li, Y.; Han, G.; He, Y.; Zhou, X.; Geng, S.; Sheng, X.; Jiang, S.; Sun, S.; Qin, C.-F.; Zhou, Y. Adaptation of SARS-CoV-2 in BALB/c Mice for Testing Vaccine Efficacy. *Science* **2020**, *369*, 1603−1607.

(16) Pulendran, B.; S. Arunachalam, P.; O'Hagan, D. T. Emerging Concepts in the Science of Vaccine Adjuvants. *Nat. Rev. Drug Discovery* **2021**, *20*, 454−475.

(17) HogenEsch, H.; O'Hagan, D. T.; Fox, C. B. Optimizing the Utilization of Aluminum Adjuvants in Vaccines: You Might Just Get What You Want. *npj Vaccines* **2018**, *3*, 51.

(18) Steinbuck, M. P.; Seenappa, L. M.; Jakubowski, A.; McNeil, L. K.; Haqq, C. M.; DeMuth, P. C. A Lymph Node-Targeted Amphiphile Vaccine Induces Potent Cellular and Humoral Immunity to SARS-CoV-2. *Sci. Adv.* **2021**, *7*, No. eabe5819.

(19) Arunachalam, P. S.; Walls, A. C.; Golden, N.; Atyeo, C.; Fischinger, S.; Li, C.; Aye, P.; Navarro, M. J.; Lai, L.; Edara, V. V.; Röltgen, K.; Rogers, K.; Shirreff, L.; Ferrell, D. E.; Wrenn, S.; Pettie, D.; Kraft, J. C.; Miranda, M. C.; Kepl, E.; Sydeman, C.; Brunette, N.; Murphy, M.; Fiala, B.; Carter, L.; White, A. G.; Trisal, M.; Hsieh, C.-L.; Russell-Lodrigue, K.; Monjure, C.; Dufour, J.; Spencer, S.; Doyle-Meyers, L.; Bohm, R. P.; Maness, N. J.; Roy, C.; Plante, J. A.; Plante, K. S.; Zhu, A.; Gorman, M. J.; Shin, S.; Shen, X.; Fontenot, J.; Gupta, S.; O'Hagan, D. T.; Van Der Most, R.; Rappuoli, R.; Coffman, R. L.; Novack, D.; McLellan, J. S.; Subramaniam, S.; Montefiori, D.; Boyd, S. D.; Flynn, J. L.; Alter, G.; Villinger, F.; Kleanthous, H.; Rappaport, J.; Suthar, M. S.; King, N. P.; Veesler, D.; Pulendran, B. Adjuvanting a Subunit COVID-19 Vaccine to Induce Protective Immunity. *Nature* **2021**, *594*, 253−258.

(20) Kohlgruber, A. C.; Donado, C. A.; LaMarche, N. M.; Brenner, M. B.; Brennan, P. J. Activation Strategies for Invariant Natural Killer T Cells. *Immunogenetics* **2016**, *68*, 649−663.

(21) Yang, G.; Schmieg, J.; Tsuji, M.; Franck, R. W. The C-Glycoside Analogue of the Immunostimulant Alpha-Galactosylceramide (KRN7000): Synthesis and Striking Enhancement of Activity. *Angew. Chem., Int. Ed.* **2004**, *43*, 3818−3822.

(22) Schmieg, J.; Yang, G.; Franck, R. W.; Tsuji, M. Superior Protection against Malaria and Melanoma Metastases by a C-Glycoside Analogue of the Natural Killer T Cell Ligand α-Galactosylceramide. *J. Exp. Med.* **2003**, *198*, 1631−1641.

(23) Miyamoto, K.; Miyake, S.; Yamamura, T. Synthetic Glycolipid Prevents Autoimmune Encephalomyelitis by Inducing TH2 Bias of Natural Killer T Cells. *Nature* **2001**, *413*, 531−534.

(24) Yu, K. O. A.; Im, J. S.; Molano, A.; Dutronc, Y.; Illarionov, P. A.; Forestier, C.; Fujiwara, N.; Arias, I.; Miyake, S.; Yamamura, T.; Chang, Y.-T.; Besra, G. S.; Porcelli, S. A. Modulation of CD1d-Restricted NKT Cell Responses by Using N-Acyl Variants of Alpha-Galactosylceramides. *Proc. Natl. Acad. Sci. U.S.A.* **2005**, *102*, 3383−3388.

(25) Kopecky-Bromberg, S. A.; Fraser, K. A.; Pica, N.; Carnero, E.; Moran, T. M.; Franck, R. W.; Tsuji, M.; Palese, P. Alpha-C-Galactosylceramide as an Adjuvant for a Live Attenuated Influenza Virus Vaccine. *Vaccine* **2009**, *27*, 3766−3774.

(26) Lee, Y.-S.; Lee, K.-A.; Lee, J.-Y.; Kang, M.-H.; Song, Y. C.; Baek, D. J.; Kim, S.; Kang, C.-Y. An α-GalCer Analogue with

https://doi.org/10.1021/acs.jmedchem.1c00881
J. Med. Chem. XXXX, XXX, XXX−XXX

Branched Acyl Chain Enhances Protective Immune Responses in a Nasal Influenza Vaccine. *Vaccine* **2011**, *29*, 417−425.
(27) Hung, J.-T.; Tsai, Y.-C.; Lin, W.-D.; Jan, J.-T.; Lin, K.-H.; Huang, J.-R.; Cheng, J.-Y.; Chen, M.-W.; Wong, C.-H.; Yu, A. L. Potent Adjuvant Effects of Novel NKT Stimulatory Glycolipids on Hemagglutinin Based DNA Vaccine for H5N1 Influenza Virus. *Antiviral Res.* **2014**, *107*, 110−118.
(28) Driver, J. P.; de Carvalho Madrid, D. M.; Gu, W.; Artiaga, B. L.; Richt, J. A. Modulation of Immune Responses to Influenza A Virus Vaccines by Natural Killer T Cells. *Front. Immunol.* **2020**, *11*, 2172.
(29) Venkataswamy, M. M.; Ng, T. W.; Kharkwal, S. S.; Carreño, L. J.; Johnson, A. J.; Kunnath-Velayudhan, S.; Liu, Z.; Bittman, R.; Jervis, P. J.; Cox, L. R.; Besra, G. S.; Wen, X.; Yuan, W.; Tsuji, M.; Li, X.; Ho, D. D.; Chan, J.; Lee, S.; Frothingham, R.; Haynes, B. F.; Panas, M. W.; Gillard, G. O.; Sixsmith, J. D.; Korioth-Schmitz, B.; Schmitz, J. E.; Larsen, M. H.; Jacobs, W. R.; Porcelli, S. A. Improving Mycobacterium Bovis Bacillus Calmette-Guèrin as a Vaccine Delivery Vector for Viral Antigens by Incorporation of Glycolipid Activators of NKT Cells. *PLoS One* **2014**, *9*, No. e108383.
(30) Li, X.; Fujio, M.; Imamura, M.; Wu, D.; Vasan, S.; Wong, C.-H.; Ho, D. D.; Tsuji, M. Design of a Potent CD1d-Binding NKT Cell Ligand as a Vaccine Adjuvant. *Proc. Natl. Acad. Sci. U.S.A.* **2010**, *107*, 13010−13015.
(31) Courtney, A. N.; Nehete, P. N.; Nehete, B. P.; Thapa, P.; Zhou, D.; Sastry, K. J. Alpha-Galactosylceramide Is an Effective Mucosal Adjuvant for Repeated Intranasal or Oral Delivery of HIV Peptide Antigens. *Vaccine* **2009**, *27*, 3335−3341.
(32) Galli, G.; Pittoni, P.; Tonti, E.; Malzone, C.; Uematsu, Y.; Tortoli, M.; Maione, D.; Volpini, G.; Finco, O.; Nuti, S.; Tavarini, S.; Dellabona, P.; Rappuoli, R.; Casorati, G.; Abrignani, S. Invariant NKT Cells Sustain Specific B Cell Responses and Memory. *Proc. Natl. Acad. Sci. U.S.A.* **2007**, *104*, 3984−3989.
(33) Huang, Y.; Chen, A.; Li, X.; Chen, Z.; Zhang, W.; Song, Y.; Gurner, D.; Gardiner, D.; Basu, S.; Ho, D. D.; Tsuji, M. Enhancement of HIV DNA Vaccine Immunogenicity by the NKT Cell Ligand, α-Galactosylceramide. *Vaccine* **2008**, *26*, 1807−1816.
(34) Bershteyn, A.; Hanson, M. C.; Crespo, M. P.; Moon, J. J.; Li, A. V.; Suh, H.; Irvine, D. J. Robust IgG Responses to Nanograms of Antigen Using a Biomimetic Lipid-Coated Particle Vaccine. *J. Controlled Release* **2012**, *157*, 354−365.
(35) Ghinnagow, R.; Cruz, L. J.; Macho-Fernandez, E.; Faveeuw, C.; Trottein, F. Enhancement of Adjuvant Functions of Natural Killer T Cells Using Nanovector Delivery Systems: Application in Anticancer Immune Therapy. *Front. Immunol.* **2017**, *8*, 879.
(36) Liu, Z.; Byun, H.-S.; Bittman, R. Synthesis of Immunostimulatory Alpha-C-Galactosylceramide Glycolipids via Sonogashira Coupling, Asymmetric Epoxidation, and Trichloroacetimidate-Mediated Epoxide Opening. *Org. Lett.* **2010**, *12*, 2974−2977.
(37) Wipf, P.; Pierce, J. G. Expedient Synthesis of the Alpha-C-Glycoside Analogue of the Immunostimulant Galactosylceramide (KRN7000). *Org. Lett.* **2006**, *8*, 3375−3378.
(38) Altiti, A. S.; Mootoo, D. R. Intramolecular Nitrogen Delivery for the Synthesis of C-Glycosphingolipids. Application to the C-Glycoside of the Immunostimulant KRN7000. *Org. Lett.* **2014**, *16*, 1466−1469.
(39) Altiti, A. S.; Bachan, S.; Mootoo, D. R. The Crotylation Way to Glycosphingolipids: Synthesis of Analogues of KRN7000. *Org. Lett.* **2016**, *18*, 4654−4657.
(40) Chen, G.; Schmieg, J.; Tsuji, M.; Franck, R. W. Efficient Synthesis of α-C-Galactosyl Ceramide Immunostimulants: Use of Ethylene-Promoted Olefin Cross-Metathesis. *Org. Lett.* **2004**, *6*, 4077−4080.
(41) Chang, Y.-J.; Hsuan, Y.-C.; Lai, A. C.-Y.; Han, Y.-C.; Hou, D.-R. Synthesis of α-C-Galactosylceramide via Diastereoselective Aziridination: The New Immunostimulant 4′-Epi-C-Glycoside of KRN7000. *Org. Lett.* **2016**, *18*, 808−811.
(42) Guillaume, J.; Seki, T.; Decruy, T.; Venken, K.; Elewaut, D.; Tsuji, M.; Van Calenbergh, S. Synthesis of C6″-Modified α-C-GalCer Analogues as Mouse and Human iNKT Cell Agonists. *Org. Biomol. Chem.* **2017**, *15*, 2217−2225.
(43) Chen, G.; Chien, M.; Tsuji, M.; Franck, R. W. E and Z Alpha-C-Galactosylceramides by Julia-Lythgoe-Kocienski Chemistry: A Test of the Receptor-Binding Model for Glycolipid Immunostimulants. *Chembiochem* **2006**, *7*, 1017−1022.
(44) Lu, X.; Song, L.; Metelitsa, L. S.; Bittman, R. Synthesis and Evaluation of an Alpha-C-Galactosylceramide Analogue That Induces Th1-Biased Responses in Human Natural Killer T Cells. *Chembiochem* **2006**, *7*, 1750−1756.
(45) Liu, Z.; Byun, H.-S.; Bittman, R. Total Synthesis of α-1C-Galactosylceramide, an Immunostimulatory C-Glycosphingolipid, and Confirmation of the Stereochemistry in the First-Generation Synthesis. *J. Org. Chem.* **2011**, *76*, 8588−8598.
(46) Zou, W.; Lacroix, E.; Wang, Z.; Wu, S.-H. Synthesis of Thio-C-Glycosides from 2′-Carbonylalkyl C-Glycosides by a Tandem β-Elimination and Intramolecular Hetero-Michael Addition. *Tetrahedron Lett.* **2003**, *44*, 4431−4433.
(47) Katsuki, T.; Sharpless, K. B. The First Practical Method for Asymmetric Epoxidation. *J. Am. Chem. Soc.* **1980**, *102*, 5974−5976.
(48) Cui, Y.; Li, Z.; Cheng, Z.; Xia, C.; Zhang, Y. 4,5-Cis Unsaturated α-GalCer Analogues Distinctly Lead to CD1d-Mediated Th1-Biased NKT Cell Responses. *Chem. Res. Toxicol.* **2015**, *28*, 1209−1215.
(49) Zhang, Y.; Guo, J.; Xu, X.; Gao, Q.; Liu, X.; Ding, N. A Practical and Scalable Synthesis of KRN7000 Using Glycosyl Iodide as the Glycosyl Donor. *J. Chem. Res.* **2020**, *45*, 248.
(50) Lu, S.-R.; Lai, Y.-H.; Chen, J.-H.; Liu, C.-Y.; Mong, K.-K. T. Dimethylformamide: An Unusual Glycosylation Modulator. *Angew. Chem., Int. Ed.* **2011**, *50*, 7315−7320.
(51) Zhang, Z.; Ollmann, I. R.; Ye, X.-S.; Wischnat, R.; Baasov, T.; Wong, C.-H. Programmable One-Pot Oligosaccharide Synthesis. *J. Am. Chem. Soc.* **1999**, *121*, 734−753.
(52) Behrens, C. H.; Sharpless, K. B. New Transformations of 2,3-Epoxy Alcohols and Related Derivatives. Easy Routes to Homochiral Substances. *Aldrichimica Acta* **1983**, *16*, 67−79.
(53) Yin, X.-G.; Chen, X.-Z.; Sun, W.-M.; Geng, X.-S.; Zhang, X.-K.; Wang, J.; Ji, P.-P.; Zhou, Z.-Y.; Baek, D. J.; Yang, G.-F.; Liu, Z.; Guo, J. IgG Antibody Response Elicited by a Fully Synthetic Two-Component Carbohydrate-Based Cancer Vaccine Candidate with α-Galactosylceramide as Built-in Adjuvant. *Org. Lett.* **2017**, *19*, 456−459.
(54) Plettenburg, O.; Bodmer-Narkevitch, V.; Wong, C.-H. Synthesis of α-Galactosyl Ceramide, a Potent Immunostimulatory Agent. *J. Org. Chem.* **2002**, *67*, 4559−4564.
(55) Seco, J. M.; Quiñoá, E.; Riguera, R. The Assignment of Absolute Configuration by NMR. *Chem. Rev.* **2004**, *104*, 17−118.
(56) Pu, J.; Franck, R. W. C-Galactosylceramide Diastereomers via Sharpless Asymmetric Epoxidation Chemistry. *Tetrahedron* **2008**, *64*, 8618−8629.
(57) Mootoo, D. R.; Fraser-Reid, B. Remote Participation in Electrophilic Reactions of 'Protected' Polyols. *J. Chem. Soc., Chem. Commun.* **1986**, *21*, 1570−1571.
(58) Ayad, T.; Génisson, Y.; Verdu, A.; Baltas, M.; Gorrichon, L. A New Diorganozinc-Based Enantioselective Access to Truncated d-Ribo-Phytosphingosine. *Tetrahedron Lett.* **2003**, *44*, 579−582.
(59) Devera, T. S.; Shah, H. B.; Lang, G. A.; Lang, M. L. Glycolipid-Activated NKT Cells Support the Induction of Persistent Plasma Cell Responses and Antibody Titers. *Eur. J. Immunol.* **2008**, *38*, 1001−1011.
(60) Kaur, R.; Chen, J.; Dawoodji, A.; Cerundolo, V.; Garcia-Diaz, Y. R.; Wojno, J.; Cox, L. R.; Besra, G. S.; Moghaddam, B.; Perrie, Y. Preparation, Characterisation and Entrapment of a Non-Glycosidic Threitol Ceramide into Liposomes for Presentation to Invariant Natural Killer T Cells. *J. Pharm. Sci.* **2011**, *100*, 2724−2733.
(61) Tang, J.; Zhang, N.; Tao, X.; Zhao, G.; Guo, Y.; Tseng, C.-T. K.; Jiang, S.; Du, L.; Zhou, Y. Optimization of Antigen Dose for a Receptor-Binding Domain-Based Subunit Vaccine against MERS Coronavirus. *Hum. Vaccines Immunother.* **2015**, *11*, 1244−1250.

https://doi.org/10.1021/acs.jmedchem.1c00881
J. Med. Chem. XXXX, XXX, XXX−XXX

(62) Fox, C. B.; Kramer, R. M.; Barnes V, L.; Dowling, Q. M.; Vedvick, T. S. Working Together: Interactions between Vaccine Antigens and Adjuvants. *Ther. Adv. Vaccines* **2013**, *1*, 7−20.
(63) Huang, Y.-L.; Hung, J.-T.; Cheung, S. K. C.; Lee, H.-Y.; Chu, K.-C.; Li, S.-T.; Lin, Y.-C.; Ren, C.-T.; Cheng, T.-J. R.; Hsu, T.-L.; Yu, A. L.; Wu, C.-Y.; Wong, C.-H. Carbohydrate-Based Vaccines with a Glycolipid Adjuvant for Breast Cancer. *Proc. Natl. Acad. Sci. U.S.A.* **2013**, *110*, 2517−2522.
(64) Du, J. J.; Zou, S. Y.; Chen, X. Z.; Xu, W. B.; Wang, C. W.; Zhang, L.; Tang, Y. K.; Zhou, S. H.; Wang, J.; Yin, X. G.; Gao, X. F.; Liu, Z.; Guo, J. Liposomal Antitumor Vaccines Targeting Mucin 1 Elicit a Lipid-Dependent Immunodominant Response. *Chem.−Asian J.* **2019**, *14*, 2116−2121.
(65) Yin, X.-G.; Lu, J.; Wang, J.; Zhang, R.-Y.; Wang, X.-F.; Liao, C.-M.; Liu, X.-P.; Liu, Z.; Guo, J. Synthesis and Evaluation of Liposomal Anti-GM3 Cancer Vaccine Candidates Covalently and Noncovalently Adjuvanted by alphaGalCer. *J. Med. Chem.* **2021**, *64*, 1951−1965.
(66) Broecker, F.; Götze, S.; Hudon, J.; Rathwell, D. C. K.; Pereira, C. L.; Stallforth, P.; Anish, C.; Seeberger, P. H. Synthesis, Liposomal Formulation, and Immunological Evaluation of a Minimalistic Carbohydrate-α-GalCer Vaccine Candidate. *J. Med. Chem.* **2018**, *61*, 4918−4927.
(67) Grifoni, A.; Weiskopf, D.; Ramirez, S. I.; Mateus, J.; Dan, J. M.; Moderbacher, C. R.; Rawlings, S. A.; Sutherland, A.; Premkumar, L.; Jadi, R. S.; Marrama, D.; de Silva, A. M.; Frazier, A.; Carlin, A. F.; Greenbaum, J. A.; Peters, B.; Krammer, F.; Smith, D. M.; Crotty, S.; Sette, A. Targets of T Cell Responses to SARS-CoV-2 Coronavirus in Humans with COVID-19 Disease and Unexposed Individuals. *Cell* **2020**, *181*, 1489−1501. e15
(68) Lang, M. L. The Influence of Invariant Natural Killer T Cells on Humoral Immunity to T-Dependent and -Independent Antigens. *Front. Immunol.* **2018**, *9*, 305.
(69) Im, J. S.; Arora, P.; Bricard, G.; Molano, A.; Venkataswamy, M. M.; Baine, I.; Jerud, E. S.; Goldberg, M. F.; Baena, A.; Yu, K. O. A.; Ndonye, R. M.; Howell, A. R.; Yuan, W.; Cresswell, P.; Chang, Y.-T.; Illarionov, P. A.; Besra, G. S.; Porcelli, S. A. Kinetics and Cellular Site of Glycolipid Loading Control the Outcome of Natural Killer T Cell Activation. *Immunity* **2009**, *30*, 888−898.
(70) Artiaga, B. L.; Whitener, R. L.; Staples, C. R.; Driver, J. P. Adjuvant Effects of Therapeutic Glycolipids Administered to a Cohort of NKT Cell-Diverse Pigs. *Vet. Immunol. Immunopathol.* **2014**, *162*, 1−13.
(71) Bertoletti, A.; Tan, A. T.; Le Bert, N. The T-Cell Response to SARS-CoV-2: Kinetic and Quantitative Aspects and the Case for Their Protective Role. *Oxf. Open Immunol.* **2021**, *2*, iqab006.
(72) Fujii, S.-i.; Shimizu, K.; Hemmi, H.; Fukui, M.; Bonito, A. J.; Chen, G.; Franck, R. W.; Tsuji, M.; Steinman, R. M. Glycolipid -C-Galactosylceramide Is a Distinct Inducer of Dendritic Cell Function during Innate and Adaptive Immune Responses of Mice. *Proc. Natl. Acad. Sci. U.S.A.* **2006**, *103*, 11252−11257.
(73) Takami, M.; Ihara, F.; Motohashi, S. Clinical Application of iNKT Cell-Mediated Anti-Tumor Activity Against Lung Cancer and Head and Neck Cancer. *Front. Immunol.* **2018**, *9*, 2021.
(74) Ishibashi, F.; Sakairi, Y.; Iwata, T.; Moriya, Y.; Mizobuchi, T.; Hoshino, H.; Yoshida, S.; Hanaoka, H.; Yoshino, I.; Motohashi, S. A Phase I Study of Loco-Regional Immunotherapy by Transbronchial Injection of α-Galactosylceramide-Pulsed Antigen Presenting Cells in Patients with Lung Cancer. *Clin. Immunol.* **2020**, *215*, 108457.
(75) Nie, J.; Li, Q.; Wu, J.; Zhao, C.; Hao, H.; Liu, H.; Zhang, L.; Nie, L.; Qin, H.; Wang, M.; Lu, Q.; Li, X.; Sun, Q.; Liu, J.; Fan, C.; Huang, W.; Xu, M.; Wang, Y. Establishment and Validation of a Pseudovirus Neutralization Assay for SARS-CoV-2. *Emerging Microbes Infect.* **2020**, *9*, 680−686.

https://doi.org/10.1021/acs.jmedchem.1c00881
J. Med. Chem. XXXX, XXX, XXX−XXX